Global Biogeochemical Cycles

RESEARCH ARTICLE
10.1029/2024GB008206

Nitrogen Biogeochemistry of Adjacent Mesoscale Eddies in the North Pacific Subtropical Gyre

Mengyang Zhou[1], Julie Granger[1], Cesar B. Rocha[2], Samantha A. Siedlecki[1], Benedetto Barone[3], and Angelicque E. White[3]

[1]Department of Marine Sciences, University of Connecticut, Groton, CT, USA, [2]Instituto Oceanográfico, Universidade de São Paulo, São Paulo, Brasil, [3]Department of Oceanography, University of Hawai'i at Mānoa, Honolulu, HI, USA

Key Points:

- Subsurface nutrients along isopycnals were higher at the edges of a cyclonic eddy than in the surroundings, indicating shallow remineralization
- Nitrate isotope ratios evidenced nitrate partial assimilation below the euphotic zone, coincident with negative preformed nutrients
- Biological N_2 fixation couldn't be inferred from $^{15}N/^{14}N$ of sinking particles compared to subsurface nitrate due to the eddies' non-steady state

Supporting Information:

Supporting Information may be found in the online version of this article.

Correspondence to:

M. Zhou,
mengyang.zhou2024@gmail.com

Citation:

Zhou, M., Granger, J., Rocha, C. B., Siedlecki, S. A., Barone, B., & White, A. E. (2025). Nitrogen biogeochemistry of adjacent mesoscale eddies in the North Pacific Subtropical Gyre. *Global Biogeochemical Cycles*, *39*, e2024GB008206. https://doi.org/10.1029/2024GB008206

Received 16 APR 2024
Accepted 7 JAN 2025

Author Contributions:

Conceptualization: Mengyang Zhou, Julie Granger, Samantha A. Siedlecki, Benedetto Barone, Angelicque E. White
Formal analysis: Mengyang Zhou, Cesar B. Rocha, Benedetto Barone
Funding acquisition: Julie Granger, Angelicque E. White
Investigation: Mengyang Zhou, Julie Granger, Cesar B. Rocha, Samantha A. Siedlecki, Benedetto Barone, Angelicque E. White
Methodology: Mengyang Zhou, Julie Granger, Cesar B. Rocha, Benedetto Barone, Angelicque E. White
Resources: Julie Granger, Angelicque E. White
Software: Mengyang Zhou
Supervision: Julie Granger, Angelicque E. White

Abstract We examined the nitrogen (N) biogeochemistry of adjacent cyclonic and anticyclonic eddies near Hawai'i in the North Pacific Subtropical Gyre (NPSG) and explored mechanisms that sustain productivity in the cyclone after the initial intensification stage. The top of the nutricline was uplifted into the euphotic zone in the cyclone and depressed in the anticyclone. Subsurface nutrient concentrations and apparent oxygen utilization at the cyclone's inner periphery were higher than expected from isopycnal displacement, suggesting that shallow remineralization of organic material generated excess nutrients in the subsurface. The excess nutrients may provide a supply of subsurface nutrients to sustain productivity in maturing eddies. The shallow remineralization also raises questions regarding the extent to which cyclonic eddies promote deep carbon sequestration in subtropical gyres such as the NPSG. An upward increase in nitrate $^{15}N/^{14}N$ isotope ratios below the euphotic zone, indicative of partial nitrate assimilation, coincided with negative preformed nutrients—potentially signaling heterotrophic bacterial consumption of carbon-rich (nitrogen-poor) organic material. The $^{15}N/^{14}N$ of material collected in shallow sediment traps was significantly higher in the cyclone than in the anticyclone and showed correspondence to the $^{15}N/^{14}N$ ratio of the nitrate supply, which is acutely sensitive to sea level anomaly in the region. A number of approaches were applied to estimate the contribution of N_2 fixation to export production. Results among approaches were inconsistent, which we attribute to non-steady state conditions during our observation period.

Plain Language Summary Mesoscale eddies are ubiquitous physical manifestations of "swirling water" throughout the ocean, equated with the "weather" of the ocean. They have distinct properties compared to their surroundings, transporting heat, salt and nutrients horizontally and vertically. Their influence on ocean ecosystems is difficult to study due to their ephemeral nature. We examined the nitrogen (N) biogeochemistry of adjacent cyclonic (counter-clockwise in the northern hemisphere) and anticyclonic (clockwise in the northern hemisphere) eddies in the North Pacific Subtropical Gyre. Nitrogen, in the form of nitrate, is an essential nutrient that promotes phytoplankton growth on the sun-lit surface. Nutrients were higher than those in the surroundings directly below the sun-lit surface of the cyclonic eddy, signaling the relatively shallow decomposition of sinking organic matter. This shallow nutrient reservoir at the subsurface may fertilize the surface of mature and decaying cyclonic eddies from mixing. The nitrate N isotope ratio signaled nitrate consumption below the sun-lit surface, potentially by non-photosynthetic microbes assimilating carbon-rich material. We had hoped to exploit depth profiles of nitrate N isotope ratios to assess the contributions of a specific microbial metabolism ("di-nitrogen fixation") to the rain of particles out of the surface; however, the disparate timing of these processes within these eddies made this exercise uncertain.

1. Introduction

Mesoscale eddies are ubiquitous features in the ocean (Chelton et al., 2011), facilitating the lateral and vertical transport of heat, salt, and nutrients (Conway et al., 2018; Dong et al., 2014; Gupta et al., 2022; Spingys et al., 2021; Zhang et al., 2014). They can trap water and biogeochemical signatures in their interior as they propagate (Chelton et al., 2011; D'Ovidio et al., 2013; Early et al., 2011; Gaube et al., 2014). The vertical motions of density surfaces in eddies influence their biogeochemistry by modulating the depth of the nutricline relative to the euphotic zone. Doming isopycnals in cyclonic eddies increase the nutrient supply to the euphotic zone, whereas deepening isopycnals in anticyclonic eddies lower the nutrient supply (Falkowski et al., 1991; Gaube et al., 2014; McGillicuddy, 2016; McGillicuddy & Robinson, 1997; McGillicuddy et al., 1998; Siegel

Validation: Mengyang Zhou, Julie Granger, Angelicque E. White
Visualization: Mengyang Zhou
Writing – original draft: Mengyang Zhou, Julie Granger
Writing – review & editing: Mengyang Zhou, Julie Granger, Cesar B. Rocha, Samantha A. Siedlecki, Benedetto Barone, Angelicque E. White

et al., 1999). The nutrient flux induced by mesoscale eddies accounts for as much as 50% of new production in the subtropical ocean (McGillicuddy et al., 1998).

The North Pacific Subtropical Gyre (NPSG) is characterized by low surface nutrients and low biomass (Karl, 1999; Karl & Church, 2017; Karl et al., 1997). Persistent thermal stratification of the upper ocean isolates the nutricline from the influence of wind mixing, impeding the delivery of nutrients into the euphotic zone (Dore et al., 2008; Letelier et al., 2004). Near Ocean Station ALOHA (A Long-term Oligotrophic Habitat Assessment, located at 22°45'N and 158°W) in the NPSG, mesoscale eddies occur during 30% of the time, driving changes in nutrient delivery and plankton community structure in the deep euphotic zone (Barone et al., 2019; Benitez-Nelson et al., 2007; Bidigare et al., 2003; Johnson et al., 2010; Letelier et al., 2000; Nicholson et al., 2008; Rii et al., 2008; Seki et al., 2001). Cyclonic eddies can stimulate primary productivity relative to the surroundings from the initial "eddy pumping" of nutrients via the shoaling of isopycnals (e.g., Falkowski et al., 1991; Siegel et al., 1999). Increased subsurface productivity persists throughout the mature and decaying stages of cyclonic eddies, ostensibly maintained by the diapycnal mixing of nutrients into the euphotic zone (Barone et al., 2022; Benitez-Nelson et al., 2007; Siegel et al., 1999).

Cyclonic eddies are also thought to promote the export of carbon to depths where CO_2 is effectively sequestered from the atmosphere, although observations corroborating this notion in subtropical gyres remain scant. In this regard, Bidigare et al. (2003) described enhanced ^{234}Th-derived carbon export in a cyclonic eddy in the lee of Hawai'i. However, a number of studies reported no increase in particulate organic material export in subtropical cyclonic eddies, but otherwise recorded enhanced silica and particulate inorganic carbon export relative to background (Barone et al., 2022; Benitez-Nelson et al., 2007; Buesseler et al., 2008; Maiti et al., 2008; Rii et al., 2008).

The stoichiometry of new and export production may also be influenced by mesoscale eddies. A characteristic feature of the NPSG (and the Sargasso Sea) is the surface drawdown of dissolved inorganic carbon that occurs in the complete absence of inorganic nutrients. The subsurface drawdown of dissolved oxygen, in turn, occurs in the absence of stoichiometrically proportional nutrient production (Abell et al., 2005; Johnson et al., 2010). Although these features are not definitively explained (e.g., Barone et al., 2022; Johnson et al., 2010; Letscher & Villareal, 2018), they may portend the surface production and shallow remineralization of carbon-rich organic material (Abell et al., 2005; Emerson & Hayward, 1995; Fawcett et al., 2018). Mesoscale eddies may modulate these stoichiometric features, potentially offering insights into their origins.

Finally, mesoscale eddies in subtropical gyres are cited to influence the magnitude of marine dinitrogen (N_2) fixation as well as the community composition of N_2 fixing organisms (Dugenne et al., 2023). The biomass of diazotrophic cyanobacteria and N_2 fixation rates are generally higher in anticyclonic eddies compared to surroundings (Davis & McGillicuddy, 2006; Liu et al., 2020; Löscher et al., 2016), including at Station ALOHA (Böttjer et al., 2017; Church et al., 2009; Davis & McGillicuddy, 2006; Dugenne et al., 2023; Fong et al., 2008; Liu et al., 2020; Löscher et al., 2016). Conversely, enhanced N_2 fixation was observed in cyclonic eddies in the Northwest Subtropical Pacific, a dynamic ascribed to excess surface phosphate and an elevated iron supply from depth (Yuan et al., 2023). N_2 fixation reportedly fuels a substantive fraction of new and export production in the NPSG (Barone et al., 2022; Böttjer et al., 2017; Karl et al., 1997). Mesoscale eddies may thus enhance export production by enhancing N_2 fixation.

Adjacent mesoscale eddies of opposite polarity were sampled as part of the MESO-SCOPE (Microbial Ecology of the Surface Ocean-Simons Collaboration on Ocean Processes and Ecology) expedition in June–July 2017 (Barone et al., 2022). Both eddies were generated in the central NPSG away from the continental margins and drifted westward (Barone et al., 2022). The cyclone and anticyclone were extreme mesoscale events relative to historical Eulerian observations at Station ALOHA (Barone et al., 2022). At the time of sampling, the cyclone was in a weakening phase, while the anticyclone was in a stable phase (Dugenne et al., 2023). The cyclone sustained higher rates of primary production in the deep euphotic zone than both the anticyclone and mean conditions at Station ALOHA (Hawco et al., 2021). The center of the cyclonic eddy hosted a more abundant community of eukaryotic phytoplankton at the deep chlorophyll maximum that resulted in larger chlorophyll concentrations, which was presumably sustained by the increased diapycnal nutrient flux (Barone et al., 2022). Nitrate and O_2 had an anomalous stoichiometry in both of the mesoscale features (Barone et al., 2022). High depth-integrated rates of N_2 fixation (670 μmol N m^{-2} d^{-1}) were observed in the anticyclone, concurrent with the onset of a *Crocosphaera* bloom (Dugenne et al., 2023).

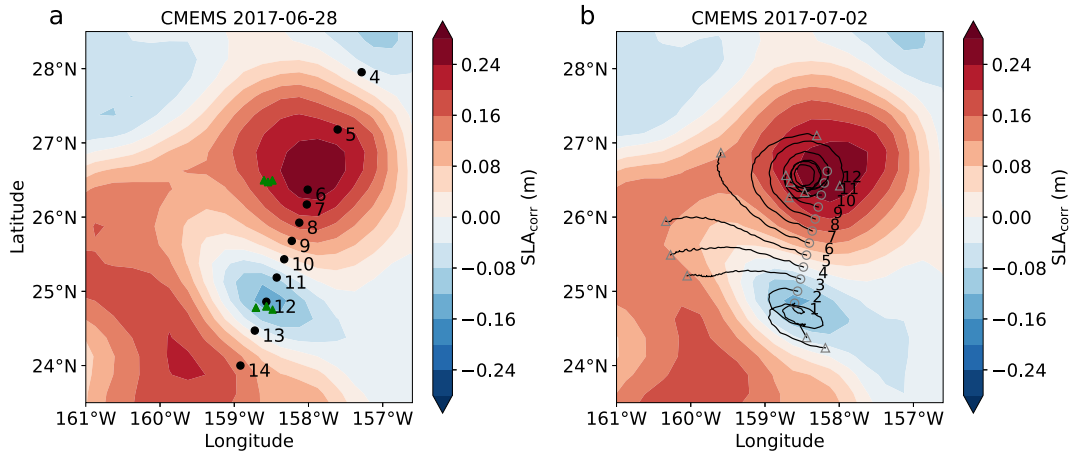

Figure 1. (a) Hydrographic stations along the transect. Contours are corrected sea level anomaly (SLA_{corr}) during the MESO-SCOPE sampling (28 June 2017). Green triangles represent locations of PAR profiles. (b) Sediment trap deployment (open circles) and recovery (triangles) positions, with lines denoting trajectories. Contours are SLA_{corr} at the time of sediment trap deployment (2 July 2017).

We obtained opportunistic samples from the campaign to characterize the stable N isotope ratios ($^{15}N/^{14}N$) of nitrate, which we interpret in the context of corresponding hydrography and biogeochemical properties. Nutrient distributions provide evidence of shallow remineralization, with implications for the mechanisms sustaining productivity in cyclonic eddies. Nitrate isotope ratios at the top of the nutricline suggest that deviations from canonical nutrient remineralization stoichiometry may derive from heterotrophic nitrate assimilation. An attempt to infer the contribution of biological N_2 fixation to the export flux from a nitrogen isotope mass balance of particles collected in shallow sediment traps relative to nitrate upwelled to the euphotic zone illustrates inherent limitations of this approach in a system that violates steady state assumptions.

2. Materials and Methods

Two eddies of opposite polarity in the north of the Hawai'i islands were surveyed during the MESO-SCOPE expedition from 26 June to 15 July 2017 near station ALOHA. A comprehensive description of the survey is detailed in Barone et al. (2022). Briefly, the eddies were identified from sea level anomaly (SLA) based on the satellite altimetry product distributed by Copernicus Marine Environment Monitoring Service (CMEMS). SLA was corrected for interannual trend and seasonal cycle, termed SLA_{corr} (Barone et al., 2019). The corrected sea level anomaly values differed by more than two standard deviations from mean values recorded at Station ALOHA between 1993 and 2018 (Barone et al., 2022). Eddies were tracked with the Mesoscale Eddy Trajectories Atlas (META3.2 delayed time all satellite version) distributed by AVISO+ (Archiving, Validation and Interpretation of Satellite Ocean data), as well as with a simplified regional tracking algorithm detailed in Barone et al. (2022).

An initial survey was conducted along a transect bisecting both eddy centers to characterize surface hydrography, which included underway conductivity, temperature, and depth measured with an underway CTD (Teledyne). Current speed and direction were measured using a hull-mounted acoustic doppler current profiler (ADCP, Workhorse 300 kHz, Teledyne). Twelve (12) water column Photosynthetically Active Radiation (PAR) profiles (Figure 1a) were measured (near local noon) near the center of the cyclone and anticyclone between July 4 and 11, 2017, using a free-falling optical profiler with data binned to 1-m intervals (Satlantic HyperPro, Sea-Bird Scientific, Bellevue, WA, USA). After the initial survey, the upper ocean biogeochemistry was characterized at 11 stations along the transect (Figure 1a) using a rosette mounted with 10 L Niskin® bottles, and profiling instruments including a CTD (Sea-Bird 911 plus), a chlorophyll fluorometer (Seapoint SCF), a polarographic O_2 sensor (SBE 43, Sea-Bird) and a transmissometer (c-star, Sea-Bird). The chlorophyll fluorometer was calibrated with chloropigment concentrations and the O_2 sensor with determinations obtained by Winkler titrations, consistent with protocols adopted by HOT (Carpenter, 1965; Tupas et al., 1997). Water samples for nutrient and nitrate isotope analyses were collected at ~25 m intervals from 5 to 500 m with higher vertical resolution (~5 m

intervals) near the deep chlorophyll maximum (DCM). Samples were frozen (−20°C) after collection pending analysis.

Twelve (12) free-drifting surface-tethered sediment traps were deployed at 150 m across the eddy centers at ∼18 km spacing to collect sinking particles. Traps were retrieved after 10–13 days (Figure 1b). The surface-tethered array included 12 individual particle interceptor trap collector tubes (Knauer et al., 1979) processed following the HOT (Hawaii Ocean Time-series) program methods (Karl & Lukas, 1996).

The concentrations of nitrate plus nitrite (N + N) and soluble reactive phosphorus (herein termed phosphate, PO_4^{3-}) were analyzed using a SEAL Autoanalyzer III using standard colorimetric protocols (Dore et al., 1996; Foreman et al., 2016). Samples with N + N concentrations less than 100 nmol L^{-1} were analyzed using a chemiluminescent method (Foreman et al., 2016).

The N isotope ratios of nitrate ($^{15}N/^{14}N$) in water samples from stations 4 to 13 were measured with the denitrifier method (Casciotti et al., 2002; Sigman et al., 2001) for concentrations exceeding 0.5 μmol L^{-1}. Nitrate was converted to nitrous oxide (N_2O) by cell concentrates of the denitrifying bacterial strain *Pseudomonas chlororaphis* (ATCC 43928, Manassas, VA, USA), which lacks the terminal N_2O reductase. The N_2O gas was extracted and purified using a custom-modified Thermo Fisher Scientific Gas Bench II fronted by dual cold traps and a GC Pal autosampler, and analyzed with a Thermo Delta V Advantage continuous flow gas chromatograph isotope ratio mass spectrometer (Casciotti et al., 2002; McIlvin & Casciotti, 2011). The N isotope ratios are expressed in delta (δ) notation in units of per mil (‰) versus a standard material (N_2 gas in the air): $\delta^{15}N_{sample} = [(^{15}N/^{14}N)_{sample}/(^{15}N/^{14}N)_{standard} - 1] \times 1000$. Nitrate isotopic analyses were calibrated to internationally recognized nitrate reference materials IAEA-NO3 (International Atomic Energy Agency, Vienna, Austria) and USGS-34 (National Institute of Standards and Technology, Gaithersburg, MD, USA) with reported $\delta^{15}N$ values of 4.7 ‰ and −1.8 ‰ (vs. air). Working solutions were diluted from primary stocks into nutrient-free seawater to concentrations bracketing sample concentrations to account for potential matrix effects (Weigand et al., 2016; M. Zhou et al., 2022). Individual samples were measured 3–9 times to achieve an analytical uncertainty to ≤0.3 ‰. The oxygen isotope ratios of nitrate ($\delta^{18}O_{NO3}$) were not measured concurrently as we did not secure sufficient sample volumes to estimate these reliably (see M. Zhou et al., 2022).

We define the mixed layer depth as the first depth where the density was 0.03 kg m^{-3} greater than the near-surface value at 10 m (de Boyer Montégut, 2004). Because PAR profiles were limited to locations near the center of the cyclone and anticyclone, we equated the DCM to the base of the euphotic zone. We note that this approximation is not entirely accurate as the average depth of the euphotic zone (defined as the depth with 1% of the surface downwelling PAR irradiance) was 103 ± 4 m in the cyclone and 108 ± 1 m in the anticyclone, whereas that of DCM was 106 ± 5 m in the cyclone, and 119 ± 6 m in the anticyclone. From the dissolved oxygen measurements, we derive the Apparent Oxygen Utilization (AOU) to discern the extent of remineralization, defined as the difference between the O_2 concentration at saturation and the observed O_2 (AOU (μmol L^{-1}) = $O_{2,\ saturation} - O_{2,\ observed}$). We also derive the concentration of preformed nitrate ($preNO_3^-$), which is the difference between the observed [N + N] and that expected from remineralization, such that $preNO_3^- = [N + N]_{observed} - AOU/R_{O2/N}$, where $R_{O2/N} = 10.5$, the stoichiometric ratio of O_2 consumption to nitrate regeneration during remineralization (Anderson, 1995).

3. Results

3.1. Physical Characteristics of the Eddies

The adjacent cyclone and anticyclone were characterized by respective shoaling (upward displacement) versus deepening (downward displacement) of isohalines and isopycnals (Figure 2a). The surface mixed layer depth varied (15–34 m) from the center of the anticyclone (station 6; 18 m) and cyclone (station 12; 34 m). Both cyclones and anticyclones were nonlinear, characterized by a ratio of rotational fluid speed (U) to translation speed (c) larger than 1, $U/c > 1$, in the upper 600 m (Text S1; Figure S1 in Supporting Information S1). In the upper 200 m, the value of U/c was >4, suggesting that the eddies trapped water within their interiors as they propagated (Figure S1 in Supporting Information S1; Chelton et al., 2011; Flierl, 1981). At the time of sampling, the cyclone was 134-day-old, and the anticyclone was 48-day-old based on the AVISO + META3.2 Delayed Time all satellites version. The regional algorithm of Barone et al. (2022) characterizes the cyclone as 240-day-old and the anticyclone as 78-day-old.

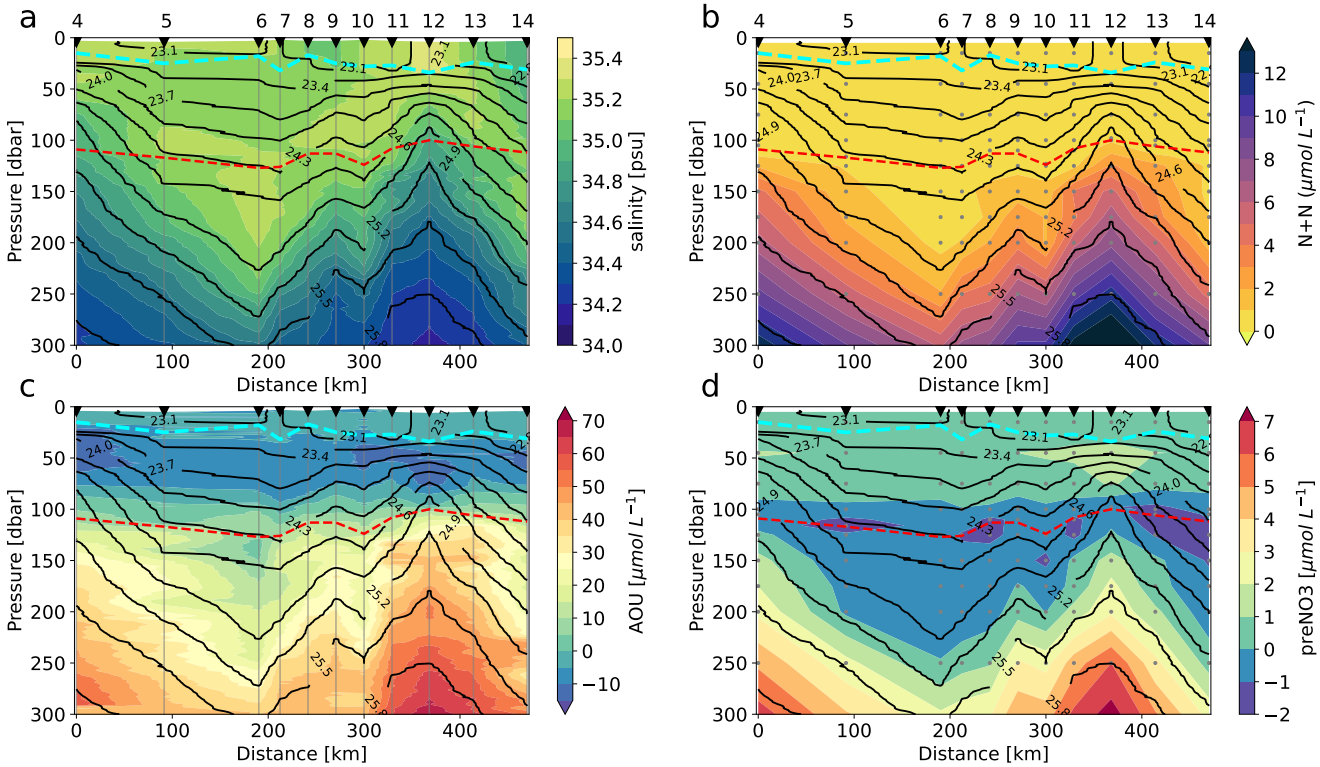

Figure 2. Depth sections along the hydrographic transect of (a) salinity, (b) N + N concentration, (c) AOU and (d) preformed nitrate ($preNO_3^-$). The contours are potential density surfaces. The red and cyan dashed lines denote the depth of the chlorophyll maximum and the depth of the mixed layer, respectively.

3.2. Biogeochemical Characteristics of the Eddies

The DCM, situated between 100–127 m among stations, was assumed to mark the base of the euphotic zone, with the shallowest DCM in the center of the cyclone and the deepest in the anticyclone (Figure 2). N + N at all stations was <0.01 μmol L^{-1} in the surface mixed layer. N + N at the DCM at the center of the cyclone (100 m) was 0.8 μmol L^{-1}, compared to <0.01 μmol L^{-1} at the DCM at the center of the anticyclone (127 m)—consistent with isopycnal displacement (Figure 2b; Figure 3a). Along the isopycnals delineated by potential density anomalies of 24.3–25.3 kg m^{-3}, [N + N] and coincident [PO_4^{3-}] were notably higher at the subsurface of the cyclonic eddy's inner edges (station 11 at 150 m and station 13 at 125–150 m)—and at the southern outer edge of the cyclone (station 14 at 125 m)—than at corresponding density horizons below the euphotic zone outside the cyclone (Figures 2b and 3a; Figure S2 in Supporting Information S1). This density horizon was otherwise uplifted above the euphotic zone at the center of the cyclone, thus depleted in [N + N] (Figure 3e). Station 10 was selected as the reference station to estimate the excess and deficit in [N + N] along the σ_θ = 24.3–25.3 kg m^{-3} isopycnal surface given its near zero SLA_{corr}. At stations 11, 13, and 14, the depth-integrated excess [N + N] was 0.03–0.1 mol N m^{-2} relative to station 10, while the depth-integrated deficit of [N + N] at the center of the cyclone (station 12) and station 4 was 0.08–0.1 mol N m^{-2}.

AOU values were negative throughout the euphotic zone due to net photosynthesis, reaching minima between 28–62 m depth at all stations (i.e., O_2 maxima), with the lowest AOU value of −17.5 μmol L^{-1} observed in the cyclone center (Figure 2c; Figure 3b). AOU increased from negative values throughout the euphotic zone (i.e., O_2 excess above saturation) to positive values below the euphotic zone (Figure 2c; Figure 3b). The highest subsurface AOU was at the center of the cyclone, and the lowest in the center of the anticyclone—consistent with isopycnal displacement. As with [N + N], AOU values along the σ_θ = 24.3–25.3 kg m^{-3} isopycnal were higher at the subsurface of the cyclone's inner edges (stations 11 and 13) and at its southern outer edge (station 14) than below the DCM at outer stations. At stations where these density horizons were otherwise uplifted into the euphotic zone, AOU along the isopycnal decreased to prominent minima at the center of the cyclone (station 12) and at station 4 due to net primary production (Figure 3f). Compared to outer station 10, excess AOU along the

10.1029/2024GB008206

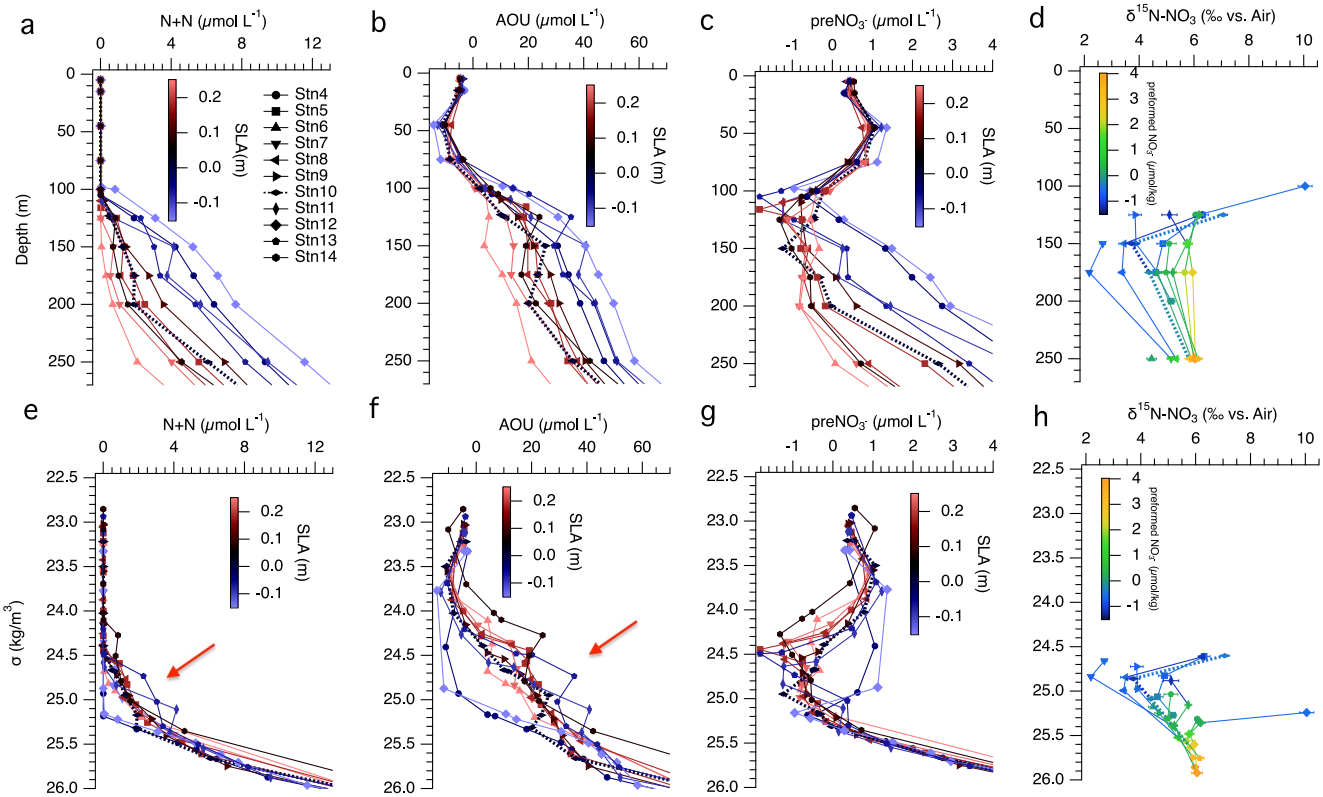

Figure 3. Shallow depth profiles at stations along the hydrographic transect of (a) N + N concentration, (b) AOU, (c) $preNO_3^-$ and (d) $\delta^{15}N_{NO3}$. Corresponding potential density profiles of (e) N + N concentration, (f) AOU, (g) $preNO_3^-$ and (h) $\delta^{15}N_{NO3}$. Colors represent corrected sea level anomaly in (a–c, e–g) and preformed NO_3^- concentration in (d, h). The red arrows in (e, f) point to the accumulation of excess nutrients along the isopycnal at the edges of the cyclone. Station 10 is shown in the dotted line.

σ_θ = 24.3–25.3 kg m^{-3} isopycnals at was 0.4–1.1 mol O_2 m^{-2} (at stations 11, 13 and 14). The excess subsurface AOU at the cyclone's inner edges showed stoichiometric correspondence to excess [N + N] (Anderson, 1995), with AOU_{excess}:N_{excess} = 10.9 ± 6.3.

The $preNO_3^-$ showed characteristic negative values at the base of the euphotic zone, ranging from −1.9 to −0.4 μmol L^{-1} in the cyclone and −1.8 to 0 μmol L^{-1} in the anticyclone (Figure 2d). Negative values at the subsurface occupied a broader depth and isopycnal intervals in the anticyclone, from the base of the euphotic zone to ~200 m (σ_θ = 24.0–25.2 kg m^{-3}) compared to ~125 m (σ_θ = 24.9–25.2 kg m^{-3}) in the cyclone. Values of $preNO_3^-$ increased with depth to positive values below the σ_θ = 25.2 kg m^{-3} isopycnal.

Depth profiles of $\delta^{15}N_{NO3}$ along transect revealed lower values at the subsurface of the anticyclone (2.5–5‰) and higher values at the subsurface cyclone (5–10‰; Figure 3d). This difference derives from a steep increase in $\delta^{15}N_{NO3}$ with potential density, as $\delta^{15}N_{NO3}$ values increased with depth, converging along density intervals (Figure 3h). Nevertheless, although subsurface values were generally lower in the anticyclone, the $\delta^{15}N_{NO3}$ values directly at the base of the euphotic zone at all stations were higher than at the subsequent depth interval—and differed among stations along isopycnals—signaling local fractionation due to partial nitrate assimilation. To isolate the assimilation signals for each depth profile, we calculated the gradients of $\delta^{15}N_{NO3}$ over depth (the difference between two adjacent $\delta^{15}N_{NO3}$ measurements divided by their depth interval). A positive $\delta^{15}N_{NO3}$ gradient represents an increase of $\delta^{15}N_{NO3}$ toward shallower depths. These assimilation signals (positive $\delta^{15}N_{NO3}$ gradients) were notably coincident with the minima in $preNO_3^-$ (i.e., negative $preNO_3^-$), where the corresponding AOU values were positive (Figure 4).

The particulate organic nitrogen (PON) fluxes collected in shallow sediment traps deployed at 150 m were comparable between the cyclonic and anticyclonic eddies, with an average value of 0.4 ± 0.1 mmol N m^{-2} d^{-1} (Figure 5a; Barone et al., 2022). The $\delta^{15}N$ of PON in sediment traps ranged from 3.0 to 4.3 ‰, with a lower range

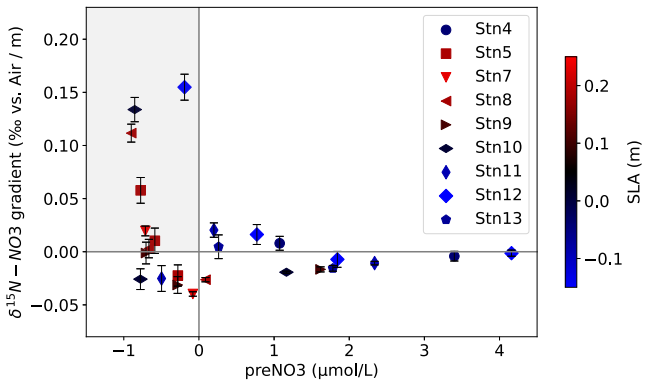

Figure 4. Depth gradients of $\delta^{15}N_{NO3}$ plotted against preNO3 with markers denoting stations and colors the corresponding corrected sea level anomaly. Positive $\delta^{15}N_{NO3}$ gradients represent upward increase of $\delta^{15}N_{NO3}$ ($\delta^{15}N_{NO3}$ increases toward shallower depths). The shaded area highlights regions of the water column where the upward increase of $\delta^{15}N_{NO3}$ coincides with negative preNO3.

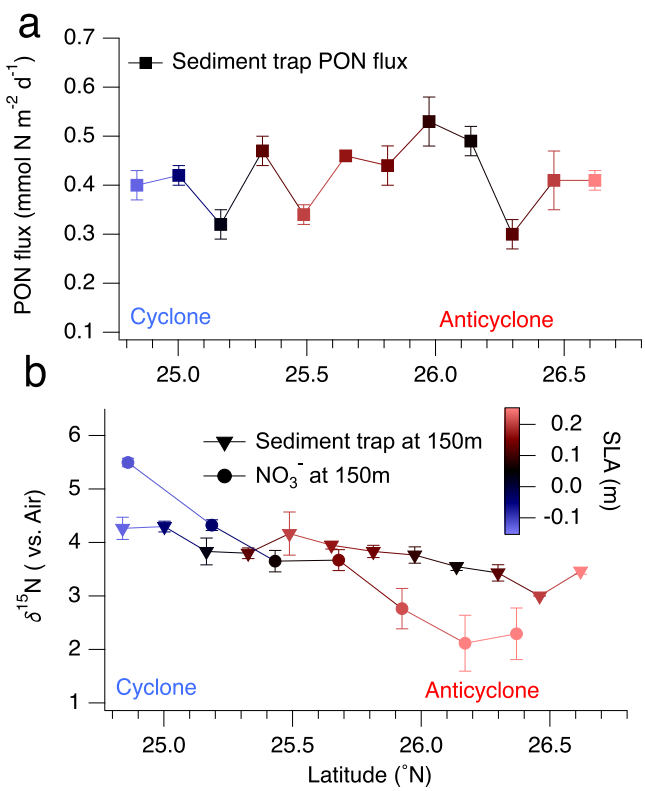

Figure 5. (a) The particulate nitrogen flux (PON) collected in sediment traps; (b) The $\delta^{15}N_{NO3}$ values at 150 m and corresponding sediment trap $\delta^{15}N_{PON}$ values plotted against latitudes along the hydrographic transect. Colors represent sea level anomaly. Error bars represent the analytical uncertainties (standard deviation) from measurement for PON flux, $\delta^{15}N_{PON}$ and $\delta^{15}N_{NO3}$. The sediment trap data are from Barone et al. (2022).

of values observed in the traps deployed in the anticyclone (3.0–4.2 ‰) compared to the cyclone (3.8–4.3 ‰; Figure 5b; Barone et al., 2022). The $\delta^{15}N_{NO3}$ values at 150 m were imprinted by the partial assimilation of nitrate (Figure 3d). To compare $\delta^{15}N_{NO3}$ values that supplied the euphotic zone with the $\delta^{15}N_{PON}$ collected in the sediment traps, we extrapolate the $\delta^{15}N_{NO3}$ to values in contiguous density horizons not influenced by partial assimilation (Figure S3 in Supporting Information S1). The resulting $\delta^{15}N_{NO3}$ at 150 m decreased from the cyclone center (5.5 ± 0.1‰) to the anticyclone center (2.3 ± 0.5‰; Figure 5b).

4. Discussion

4.1. Origin of Subsurface Nutrients

The physical and biogeochemical properties of the cyclone and anticyclone showed characteristics shared by regional eddies (Ascani et al., 2013; Barone et al., 2022; Church et al., 2009; Gaube et al., 2013; Seki et al., 2001; Xiu & Chai, 2020). DCM was shallower in the cyclone and had higher fluorescence and chlorophyll-a concentrations. Primary productivity in the deep euphotic zone was coherently higher in the cyclone (Hawco et al., 2021). Depth-integrated O_2 concentrations in the euphotic zone were higher in the cyclone than in the anticyclone.

The enhanced primary production observed in the lower euphotic zone of the cyclone center was ostensibly sustained by a greater vertical nutrient supply from diapycnal mixing; The vertical displacement of isopycnals associated with the mesoscale features resulted in higher nutrient concentrations directly below the euphotic zone of the cyclone compared to the anticyclone, borne of a steep gradient in nutrient concentrations with density (Barone et al., 2022). The gradient of the regional nutricline is explained by the incidence of Subtropical Salinity Maximum Water (STSMW; σ_θ = 24.2 kg m^{-3}) at the base of the euphotic zone (Figure 6), which is depleted of nutrients at its origin near the subtropical front (25°–30°N; Casciotti et al., 2008; Sabine et al., 1995; Tsuchiya, 1968). Nutrients therein derive in part from diapycnal mixing with underlying Shallow Salinity Minimum Water (SSMW; σ_θ = 25.8 kg/m^3) formed in the northeastern subtropical gyre, which overlies North Pacific Intermediate Water (NPIW; σ_θ = 26.8 kg m^{-3}; Talley, 1985, 1993). The low $\delta^{15}N_{NO3}$ in STSMW (as low as 2.2 ± 0.1 ‰ in the anticyclone) relative to deeper waters suggests that nitrate therein also originated from the remineralization of newly fixed N (Casciotti et al., 2008; Knapp et al., 2018). The $\delta^{15}N_{NO3}$ in NPIW at intermediate depths is ca. 7.1 ‰ (Casciotti et al., 2008; Lehmann et al., 2018; Sigman et al., 2009). The $\delta^{15}N_{NO3}$ in SSMW above is 5.6 ‰, intermediate between NPIW and STSMW. The upward decrease in $\delta^{15}N_{NO3}$ is consistent with the addition of newly fixed N from the remineralization of organic material with a nominal $\delta^{15}N$ value of −2–0 ‰ (Carpenter et al., 1997; Delwiche et al., 1979; Hoering & Ford, 1960; Minagawa & Wada, 1986) integrated over the residence time of the water mass since it was ventilated (Casciotti et al., 2008; Liu et al., 1996). The low subsurface $\delta^{15}N_{NO3}$ could additionally result from isotope fractionation during remineralization, as bacteria preferentially degrade ^{14}N, leading to a relatively low $\delta^{15}N_{NO3}$ of the remineralized nitrate (Altabet, 1988; Casciotti et al., 2008)—a notion to which we return in a later section. Directly at the base of the euphotic zone, the sharp increases in $\delta^{15}N_{NO3}$ compared to corresponding values along isopycnals are consistent with isotope fractionation due to the partial assimilation of nitrate (e.g., Fawcett et al., 2015; Lehmann et al., 2018).

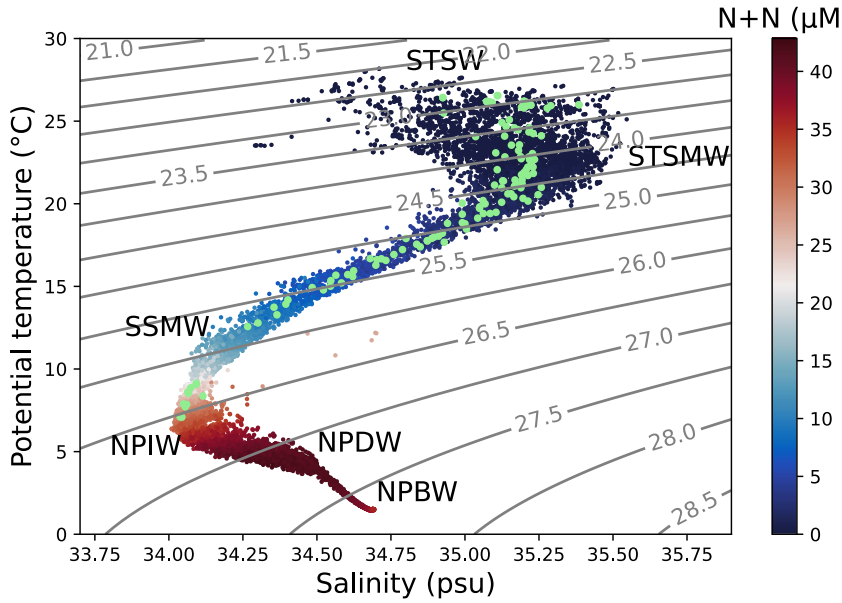

Figure 6. Potential temperature versus salinity from bottle data spanning the 30-year time series at Station ALOHA, with contours of potential density and colors of N + N concentrations. Observations of the two eddies in this study are in green. Labeled water masses include Subtropical Surface Water (STSW), Subtropical Salinity Maximum Water (STSMW), Shallow Salinity Minimum Water (SSMW), North Pacific Intermediate Water (NPIW), North Pacific Deep Water (NPDW), and North Pacific Bottom Water (NPBW). The data are from The Hawaii Ocean Time-series observations (http://hahana.soest.hawaii.edu/hot/hot-dogs/).

Away from the center at peripheral stations inside the cyclone, nutrient concentrations were even higher than along corresponding density horizons outside the eddy (and higher than the mean conditions at $\sigma_\theta \approx 25.0$ kg m^{-3} from the Station ALOHA climatology; Figure S4 in Supporting Information S1), suggesting shallow remineralization within the cyclone. The excess [N + N] along isopycnals in the cyclone was associated with a corresponding stoichiometric excess in AOU, suggesting that these signals derived proximately from shallow remineralization within the eddy. A related feature was observed by Buesseler et al. (2008) in a cyclonic eddy in the North Atlantic Subtropical Gyre, where excess thorium-234 was focused directly below the DCM.

The excess [N + N] along isopycnals could result from the shallow remineralization of the vertical flux of sinking particles generated in lighter density horizons that were uplifted into the euphotic zone directly above. Alternatively, the correspondence of excess subsurface nutrients at the cyclone's inner edges with the isopycnal uplifted into the euphotic zone in the center of the cyclone leads us to postulate that the excess remineralized nutrients could have arisen from particles exported along isopycnals (Boyd et al., 2019)—thus adding to the incident nutrient reservoir. Small sinking particles from the euphotic zone may attain neutral buoyancy at fringing isopycnals, preventing export to further depths (McCave, 1975; Omand et al., 2020; Washburn et al., 1989). We observed no evidence of shallow suspended particles from beam transmission and attenuation coefficients (data not shown), although shallow remineralization could have occurred primarily before the occupation. Otherwise, particles generated in the uplifted isopycnal in the cyclone center may have been advected tangentially toward the edges of the eddy (Gaube et al., 2013; K. Zhou et al., 2020) and then exported gravitationally. Particles may also be subducted to the subsurface along isopycnals via submesoscale fronts at the cyclone edges (Guidi et al., 2012; Lévy et al., 2012; Omand et al., 2015; Resplandy et al., 2019; Stukel et al., 2017), particularly during the intensification stage of the eddies (Guo et al., 2024). Regardless of the mechanism(s) resulting in the accrual of excess nutrients at the subsurface, this feature was not evident below the euphotic zone of the anticyclone, wherein [N + N] and AOU values were similar to those at out-stations along corresponding density horizons.

At the center of the cyclonic eddy, the uplifted isopycnals resulted in a larger nutrient reservoir directly below the euphotic zone than mean conditions, leading to a proportionally greater flux of nutrients into the euphotic zone from turbulent mixing across isopycnals—providing a means for the cyclonic eddy to remain productive after the initial isopycnal uplift into the euphotic zone (Barone et al., 2022). The so-called “eddy-pumping” of nutrients

(Falkowski et al., 1991; McGillicuddy et al., 1998) borne of the uplift of isopycnals occurred before the onset of the field survey, and was thus not captured. Barone et al. (2022) estimated a diapycnal N flux directly across the top of the nutricline of 0.08 mmol N m^{-2} d^{-1} in the cyclone and 0.009 mmol N m^{-2} d^{-1} in the anticyclone. These values are appreciably lower than the diapycnal flux estimated by Benitez-Nelson et al. (2007) of 0.32–0.51 mmol N m^{-2} d^{-1} at the center of a cyclonic eddy on the lee side of the Hawaiian islands—a difference deriving largely from the assumption of a greater diapycnal diffusivity of 5–8 × 10^{-5} m^2 s^{-1} versus that of 1.1 × 10^{-5} m^2 s^{-1} assumed by Barone et al. (2022). The estimated diapycnal flux in the cyclone is also lower than the corresponding PON sinking flux estimated from the sediment traps, which was 0.4 ± 0.03 mmol N m^{-2} d^{-1} (Barone et al., 2022).

In addition to mixing across isopycnals, mixing along isopycnals may also provide an important conduit of nutrients into the euphotic zone of the cyclone (Cao et al., 2024; Freilich & Mahadevan, 2019). Subsurface nutrients along the $\sigma_\theta \approx 25.0$ kg m^{-3} isopycnal were apt to mix into the uplifted center of the cyclone where nutrients were depleted. We estimate the isopycnal mixing flux in the cyclone and anticyclone for a diffusivity, k_{iso}, of 1 m^2 s^{-1} (Okubo, 1971; Shcherbina et al., 2015). To this end, we first compute the volume-specific flux $F_{iso,vol}$ (mmol N m^{-3} d^{-1}) from $F_{iso,vol} = k_{iso}(\partial^2 N/\partial x^2 + \partial^2 N/\partial y^2)$ where x and y are the respective zonal and meridional directions. Assuming symmetric eddies, we derive the isopycnal flux along the hydrographic transect, $F'_{iso,vol} = k_{iso}(2\partial^2 N/\partial x'^2)$, where x' is the direction along the transect. The volumetric flux, $F'_{iso,vol}$ integrated over the depth range of density σ_θ = 24.6–25.4 kg m^{-3}, yields an isopycnal flux of 0.002 mmol N m^{-2} d^{-1} in the center of the cyclone, compared to −0.0003 mmol N m^{-2} d^{-1} in the center of the anticyclone. The isopycnal mixing flux of N thus appears to be one order of magnitude lower than the diapycnal mixing flux. We note that our calculation may underestimate isopycnal fluxes because the horizontal resolution of the measurements was relatively coarse, with distances between the cyclone center and its peripheral stations of ≥38 km. Excess subsurface nutrients accrued in closer proximity to the cyclone center would result in a steeper along-isopycnal concentration gradient. For example, given a similar nutrient gradient along an arbitrary distance of 10 km (along the x' direction) from the cyclone center, isopycnal mixing would result in a flux of 0.04 mmol N m^{-2} d^{-1}, of the same order of magnitude as the diapycnal flux. This hypothesis is supported by a recent investigation of energetic submesoscale dynamics in a long-lived cyclonic eddy that revealed significant isopycnal fluxes of nutrients to the DCM (Cao et al., 2024). We thus submit that isopycnal mixing may be a means by which production is sustained beyond the initial "eddy injection."

We further attempt to quantify the remineralization fluxes that contributed to the excess nutrients in the cyclonic eddy, and compare these to the observed PON sinking fluxes and estimated diapycnal and isopycnal mixing fluxes. We make the simplified assumption that the excess nutrients at the edge of the cyclone accumulated from a constant remineralization flux during the lifetime of the eddy, acknowledging that this flux was ostensibly not constant. Given excess NO_3^- at Stations 11, 13, and 14 of 0.03–0.1 mol N m^{-2}, the time-averaged remineralization flux is on the order of 0.2–0.7 mmol N m^{-2} d^{-1} if the cyclonic eddy was 134-days-old at the time of sampling based on the AVISO + data product (0.1–0.4 mmol N m^{-2} d^{-1} if the cyclone was 240-days-old based on Barone et al. (2022)). This remineralization flux is relatively high compared to the sum of the estimated diapycnal and isopycnal nutrient fluxes of 0.08 mmol N m^{-2} d^{-1} at the time of sampling. In turn, the PON sinking flux estimated from the sediment traps in the cyclone was 0.4 ± 0.03 mmol N m^{-2} d^{-1} (Barone et al., 2022), which is comparable to our estimate of the time-averaged shallow excess remineralization flux. This calculation illustrates that the shallow excess remineralization flux is substantive. It notably contributes an additional export flux not captured by sediment traps at 150 m, given that excess nutrients are focused above this depth interval. It also shows that the nutrient flux supplied to the surface remains too low to explain the corresponding sinking PON flux, notwithstanding this additional shallow remineralization flux. This apparent inconsistency suggests that the shallow remineralization flux may derive from enhanced production fueled by the initial isopycnal uplift.

In all, our observations suggest that a substantive fraction of the particulate organic material generated in the euphotic zone was remineralized directly below the euphotic zone. Given the cyclone's nonlinear nature, remineralized nutrients were retained within the eddy and accrued at the subsurface. Remineralized nutrients at shallow depths directly below the euphotic zone were then apt to be re-supplied to the euphotic zone, allowing the cyclonic eddy to sustain primary production in the deep euphotic zone beyond that fueled by the initial uplift of isopycnals. Such "rejuvenation" of nutrients was actualized in eddy-resolving simulations of the Northern Canary upwelling system, wherein the PON generated at the surface of long-lived mesoscale eddies was largely remineralized at the shallow subsurface and re-supplied to the euphotic zone on timescale of ∼1.5 months—thus

rejuvenating multiple times over the lifetime of long-lived (∼14 months) cyclonic eddies (Lovecchio et al., 2022). While increased primary productivity in cyclonic eddies is initiated during their intensification (e.g., Guo et al., 2024), higher productivity than the surrounding may be sustained thereon by the re-supply of nutrients accrued from remineralization at the shallow subsurface.

The excess nutrients observed here were focused between 125 and 150 m, depths shallower than the sediment traps, suggesting that a sizable fraction of the export flux in the cyclone was remineralized above the traps. This fraction of the exported production from the cyclone manifestly did not reach depths where carbon is effectively sequestered away from the atmosphere (DeVries et al., 2012; DeVries & Weber, 2017). This inference conforms to the notion that warmer waters promote shallower remineralization of labile organic material (Marsay et al., 2015). It is also consistent with inverse model analyses suggesting that the transfer efficiency of sinking organic particles to the ocean interior is relatively low in subtropical gyres (Weber et al., 2016). Particle remineralization and fragmentation were recently shown to be enhanced at the DCM inside a decaying cyclonic eddy in the oligotrophic South China Sea, leading to weak carbon export (Zhu et al., 2023). Much of the enhanced production during the maturing and decaying stages of regional cyclonic mesoscale eddies may be subject to shallow remineralization, such that the remineralized carbon will resurface on sub-annual to decadal time scales.

Surprisingly, the organic particulate flux recorded in the sediment traps at 150 m was of similar magnitude in the cyclonic versus anticyclonic eddy in terms of both PON and POC, on the order of 0.4 ± 0.1 mmol N m^{-2} d^{-1} for PON—whereas particulate inorganic carbon and particulate silicate fluxes were notably greater in the cyclone (Barone et al., 2022). Similar observations in subtropical gyres have led to the conclusion that regional cyclonic eddies function as effective silica pumps but inefficient organic carbon pumps (Benitez-Nelson et al., 2007; Buesseler et al., 2008; Maiti et al., 2008; Rii et al., 2008; K. Zhou et al., 2020; Zhu et al., 2023). Barone et al. (2022) nevertheless posited that organic material produced in the cyclone during the initial isopycnal uplift was exported to deeper waters prior to the sampling campaign. In this regard, examination of multiple eddies in the NPSG revealed that carbon and nitrogen flux anomalies were negatively correlated to the eddy age, with higher export anomalies occurring during early maturity (K. Zhou et al., 2021). Guo et al. (2024) similarly observed enhanced POC export during the intensifying stage of a cyclonic eddy, a high percentage of which was transferred to the base of the mesopelagic layer. A recent survey of regional eddies further revealed that O_2 minima at mid-depths (between 600 and 900 m) were generally more prominent in cyclonic eddies than in surrounding waters, while less prominent in anticyclonic eddies, suggesting greater export to mid-depths in cyclonic eddies (Xiu & Chai, 2020). While organic material exported from the cyclone surface was ostensibly remineralized directly below the euphotic zone, the export of organic carbon to mid-depths may nevertheless have been greater in the cyclone than the anticyclone over their respective lifetimes.

4.2. Stoichiometric Anomalies at the Subsurface

A salient subsurface feature in subtropical gyres is the incidence of so-called "negative" preformed nutrients (Emerson & Hayward, 1995; Fawcett et al., 2018; Johnson et al., 2010). Given adherence to Redfield stoichiometry, negative preformed nutrients may signal the respiration of O_2 (and organic carbon) without the commensurate remineralization of nutrients, or the consumption of nutrients without the proportional production of O_2 during photosynthesis (Abell et al., 2005; Emerson & Hayward, 1995). This feature could result, at least partially, from nutrient transport by migrating plankton (Johnson et al., 2010; Letscher & Villareal, 2018; Villareal et al., 1999). Negative pre-formed nutrients may also arise from the entrainment and decomposition of N-poor dissolved organic matter from the surface and/or from the gravitational flux and remineralization of C-rich gel-like organic matter (aka, transparent exopolymer). The respiration of N poor material may, in turn, instigate heterotrophic nitrate assimilation (Abell et al., 2005; Emerson & Hayward, 1995; Fawcett et al., 2018; Letscher et al., 2015; Smyth & Letscher, 2023). Specifically, heterotrophic bacteria can fractionate nitrate isotope ratios during its assimilation (Granger et al., 2010). In this regard, Fawcett et al. (2018) showed that dark incubations of subsurface seawater in the North Atlantic Subtropical Gyre resulted in heterotrophic bacterial growth, the drawdown of incident nitrate, and a commensurate increase in nitrate isotope ratios. Moreover, seasonal increases in the $^{18}O/^{16}O$ ratio of subsurface nitrate at the Bermuda Atlantic Time Series site also suggested that heterotrophic nitrate assimilation may be required for the remineralization of C-rich and N-poor organic matter (Fawcett et al., 2018). The upward increases in $\delta^{15}N_{NO3}$ values observed here occurred below the euphotic zone, signaling the partial assimilation of nitrate at the subsurface (Figure 4). Their association with the extrema in negative

preNO$_3^-$ leads us to posit that they arise from nitrate assimilation by heterotrophic bacteria decomposing the C-rich and N-poor organic matter.

4.3. N Isotope Mass Balance to Infer N_2 Fixation in Mesoscale Eddies

New and export production in the NPSG are cited to be fueled in part by biological N_2 fixation (Karl et al., 1997). Incubation-based estimates of N_2 fixation in the euphotic zone from the HOT time series average of 230 ± 136 μmol N m^{-2} d^{-1} (Böttjer et al., 2017) for measurements made between 2005 and 2013. These may be biased by a number of methodological artifacts that have been uncovered in recent years (Dabundo et al., 2014; Mohr et al., 2010; White et al., 2020); Albeit, the potential for these biases to be evident was considered in Böttjer et al. (2017) and more recent measurements have found rates were found to be similar or higher than previously reported (Dugenne et al., 2023). Independent estimates of the contribution of N_2 fixation to export production cover a broad range, from negligible to nearly 50% of N exports (Barone et al., 2022; Böttjer et al., 2017; Casciotti et al., 2008; Dore et al., 2002; Karl et al., 1997; Mahaffey et al., 2008). The latter is derived from mass balance exercises where the $\delta^{15}N$ of sinking material recovered in shallow sediment traps is compared to the $\delta^{15}N_{NO3}$ supplied to the euphotic zone to infer the fraction of export flux from biological N_2 fixation (Altabet, 1988; Barone et al., 2022; Böttjer et al., 2017; Casciotti et al., 2008; Karl et al., 1997; Knapp et al., 2005, 2008, 2016; Mahaffey et al., 2008). The higher range of these estimates presumed a relatively enriched $\delta^{15}N_{NO3}$ end-member akin to that in intermediate depth waters, lacking direct measurements of $\delta^{15}N_{NO3}$ at shallower depths (Karl et al., 1997).

The incubation-based N_2 fixation rates estimated during the deployment were substantially higher in the anticyclone (670 μmol N m^{-2} d^{-1}) than in the cyclone (115 μmol N m^{-2} d^{-1}; Dugenne et al., 2023)—a dynamic that may be expected to manifest in the $\delta^{15}N$ of the sinking flux. The high-resolution $\delta^{15}N_{NO3}$ profiles measured here allow us to constrain the $\delta^{15}N_{NO3}$ supplied to the euphotic zone, and evaluate whether these values can be exploited to estimate the contribution of biological N_2 fixation to shallow particle export in the respective mesoscale eddies. The $\delta^{15}N$ of particulate material collected in shallow sediment traps deployed at 150 m ranged from 3.0–4.2 ‰ in the anticyclone compared to 3.8–4.3 ‰ in the cyclone (Figure 5b; Barone et al., 2022). We presume here that the $\delta^{15}N_{NO3}$ values at 150 m (the depth of sediment traps) corresponded to the nitrate supplied to the euphotic zone. Because some of these values were imprinted by the partial assimilation of nitrate, we extrapolate the $\delta^{15}N_{NO3}$ to values in contiguous density horizons not influenced by partial assimilation (Figure 5b and Figure S3 in Supporting Information S1). At corresponding stations along the transect, the $\delta^{15}N_{PON}$ values of material recovered in sediment traps in the cyclone were lower than the $\delta^{15}N_{NO3}$ values at 150 m, whereas the $\delta^{15}N_{PON}$ values of particles collected in the anticyclone were higher than the $\delta^{15}N_{NO3}$ values at 150 m (Figure 5b). Assuming the $\delta^{15}N_{NO3}$ of newly fixed N is 0 ± 1 ‰, the contribution of N_2 fixation to export production consequently inferred for the cyclonic eddy is on the order of 13 ± 3%, whereas that for the anticyclonic eddy yields a negative value of −29 ± 14%. Alternative assumptions to characterize the $\delta^{15}N_{NO3}$ of the upward nitrate flux yield similarly confounding results (Text S2; Table S1; Figure S5 in Supporting Information S1). These results are clearly problematic arising because mesoscale eddies are not a steady-state system with respect to the nutrient supply to the surface and the coincident export of organic material therefrom. The regional $\delta^{15}N_{NO3}$ gradient with density (and depth) is remarkably steep—notably steeper than that near Bermuda in the North Atlantic Subtropical Gyre (Knapp et al., 2005)—rendering the $\delta^{15}N_{NO3}$ supplied to the euphotic zone highly sensitive to SLA. The SLA in mesoscale eddies changes on relatively short time scales, such that the sinking material captured in the traps was not necessarily produced from the nitrate (and associated $\delta^{15}N_{NO3}$) co-located at the base of the euphotic zone.

We nevertheless exploit the coherence of $\delta^{15}N_{NO3}$ along isopycnals to infer the mean depth-distribution of $\delta^{15}N_{NO3}$ at Station ALOHA. The σ_θ = 24.8 kg m^{-3} isopycnal is that which commonly resides at 150–175 m depth, and has a $\delta^{15}N_{NO3}$ of 3.1 ± 0.4 ‰. The mean $\delta^{15}N_{PON}$ of sinking particles recovered monthly in sediment traps at Station ALOHA for 31 years was 3.3 ± 1.0 ‰, squarely in the $\delta^{15}N_{NO3}$ range of σ_θ = 24.8 kg m^{-3} isopycnal. Given no detectable secular change in the $\delta^{15}N_{PON}$ of sinking particles over this time (Figure S6 in Supporting Information S1), and presuming no change in the corresponding $\delta^{15}N_{NO3,}$ the fractional contribution of N_2 fixation to export production thus estimated is within the margin of error, −6 ± 35%—rendering this estimate uncertain. In contrast, Knapp et al. (2018) reported that the material captured in shallow sediment traps in the southwestern Pacific had $\delta^{15}N$ values of 0.6 ± 1 ‰, compared to subsurface $\delta^{15}N_{NO3}$ values of 7.0–8.4 ‰,

arguing for an unambiguous contribution of newly fixed N to the sinking flux, corroborating markedly elevated incubation-based estimates of N_2 fixation at this site.

The similarity of the long-term $\delta^{15}N$ average of sinking flux compared to mean $\delta^{15}N_{NO3}$ at subsurface is perplexing in light of the magnitude of in situ estimates of biological N_2 fixation at Station ALOHA. For a net regional community production of 287 ± 100 mmol N m^{-2} y^{-1} (Johnson et al., 2010), the corresponding contribution of N_2 fixation to the export flux is 29 ± 20% for a N_2 fixation rate of 230 ± 136 μmol N m^{-2} d^{-1} (Böttjer et al., 2017), which should result in a difference of at least ∼1% of sinking flux from the N isotope mass balance for a N_2-fixation endmember of 0 ‰. Based on the fact that biological N_2 fixation contributes significantly to new production at Station ALOHA, the discrepancy could arise if newly fixed N accumulates as DON in the euphotic zone. This premise was queried by Knapp et al. (2005) in the Sargasso Sea, wherein the $\delta^{15}N$ of DON in the euphotic zone was not detectably lower than at depth—noting that N_2 fixation is not thought to contribute substantively to the export flux in this region (Altabet, 1988; Knapp et al., 2008). Similarly, the $\delta^{15}N$ of DON measurements in the euphotic zone near Hawai'i did not show evidence for low $\delta^{15}N$ accumulating in the DON pool (Knapp et al., 2011). The particulate flux of newly fixed N at Station ALOHA may otherwise be episodic and thus not well aliased by shallow trap deployments (Karl et al., 2012). Alternatively, newly fixed N may remain associated with prokaryotic microbes on the premise that eukaryotes rely predominantly on nitrate (Fawcett et al., 2011); the former may be exported and remineralized at shallower depths than the sediment traps. Finally, we note that estimates of the supply of new nitrate to the surface of the NPSG are uncertain (e.g., Johnson et al., 2010) and may thus be under-estimated, rendering N_2 fixation proportionally less important.

Another uncertainty regarding the N isotope mass balance that warrants consideration is that it may be biased by isotopic fractionation during particle remineralization (Lehmann et al., 2002). Casciotti et al. (2008) observed a shift in the $\delta^{15}N$ of sinking PON near station ALOHA, from 2.5 ‰ at 150 m to 3.5 ‰ at 300 m, attributed to isotope fractionation during remineralization. Given sizable remineralization occurring above 150 m, the preferential production of low $\delta^{15}N$ nitrate from remineralization would result in the capture of PON at 150 m with a higher $\delta^{15}N$ than exited from the euphotic zone—leading to an under-estimation of the contribution of biological N_2 fixation to the PON flux. The $\delta^{15}N$ increase in sinking PON with depth could also conceivably reflect the differential export of respective plankton groups assimilating different N sources hypothesized above (e.g., Fawcett et al., 2011) and/or the depth-sensitive disaggregation and repackaging of sinking particles (e.g., Briggs et al., 2020; Lampitt et al., 1990; Wilson et al., 2008). In a parallel vein, the low $\delta^{15}N$ nitrate at the base of the euphotic zone throughout the NPSG could arise from the remineralization of suspended PON (Hannides et al., 2013) rather than the remineralization of newly fixed N. In light of the potential limitations of the N isotope mass balance approach used here, we submit that nitrate isotope ratios can provide a more robust accounting of the input of newly fixed N to the regional nitrate inventory when considering the whole of intermediate water column wherein bulk remineralization occurs (e.g., Casciotti et al., 2008; Knapp et al., 2008; Marconi et al., 2017; Marshall et al., 2022; Marshall et al., 2023) - rather than an N isotope mass balances restricted to the top of the nutricline.

5. Conclusions

Our analysis reveals that the increased production in the cyclone was patently remineralized at the cyclone edges, directly below the euphotic zone—rather than exported to depths where CO_2 is effectively sequestered. This material was remineralized at depths above the sediment traps, potentially explaining the similarity of the POC and PON export fluxes between the cyclonic and anticyclonic eddies. The shallow nutrient reservoir borne by remineralization within the eddy may provide a means to fuel primary production in mature and decaying stages of cyclonic eddy from cross-isopycnal (and potentially along-isopycnal) mixing of nutrients—promoting the continuous "rejuvenation" of nutrients over the lifetime of the eddy.

The coincidence of a subsurface nitrate assimilation signal (from $\delta^{15}N_{NO3}$) with negative preformed nutrients supports the notion that the deviations from canonical elemental stoichiometry may arise from the shallow export and remineralization of C-rich material, promoting the assimilation of nitrate by heterotrophic bacteria.

Substantially higher biological N_2 fixation was detected in the anticyclone (Dugenne et al., 2023), yet this dynamic was not discernible from the $\delta^{15}N_{PON}$ of sinking particles recovered in sediment traps compared to the nitrate $\delta^{15}N_{NO3}$ at 150 m due to the non-steady state nature of the system. A steep isopycnal gradient of nitrate $\delta^{15}N_{NO3}$ renders subsurface values sensitive to SLA, such that the $\delta^{15}N_{PON}$ along transect mirrored corresponding

differences in the $\delta^{15}N_{NO3}$ of the nitrate that fueled new production. Averaged over long timescales, the N isotope mass balance of the euphotic zone did not appear sensitive to the export flux of newly fixed N at Station ALOHA for reasons that remain unclear.

Our study highlights the need to better characterize the physical mechanisms of nutrient delivery to the surface oligotrophic ocean, particularly in light of increased surface ocean stratification (Li et al., 2020; Polovina et al., 2008; Sallée et al., 2021). Studies that achieve high vertical and horizontal resolution of mesoscale features will allow for better characterization of the fate of export production based on the subsurface nutrient reservoir. Our study also impels consideration of how to better constrain the significance of N_2 fixation to the export flux in the NPSG.

Data Availability Statement

Nitrate $\delta^{15}N_{NO3}$ measurements in this study are archived on Zenodo (M. Zhou et al., 2025). Hydrographic and biogeochemical measurements can also be found on Zenodo (Barone et al., 2021). Data were obtained via the Hawaii Ocean Time-series HOT-DOGS application (University of Hawai'i at Mānoa. National Science Foundation Award # 2241005) can be found at HOT-DOGS (2024). The altimetric Mesoscale Eddy Trajectories Atlas (META3.2 DT) was produced by SSALTO/DUACS and distributed by AVISO+ with support from CNES, in collaboration with IMEDEA (Pegliasco et al., 2022).

Acknowledgments
The authors thank D. Karl for insightful comments on the manuscript. We also thank an anonymous reviewer for insightful comments that improved the manuscript. The authors are grateful to V. Rollinson and P. Ruffino for their technical assistance with mass spectrometry analyses. This work was supported by CAREER award to J.G. from the US National Science Foundation Division of Ocean Sciences (OCE-1554474) and by the Simons Collaboration on Ocean Processes and Ecology program (#329104 to A.W.), which supported the field sampling effort.

References

Abell, J., Emerson, S., & Keil, R. G. (2005). Using preformed nitrate to infer decadal changes in DOM remineralization in the subtropical North Pacific. *Global Biogeochemical Cycles*, *19*, 1–16. https://doi.org/10.1029/2004GB002285

Altabet, M. A. (1988). Variations in nitrogen isotopic composition between sinking and suspended particles: Implications for nitrogen cycling and particle transformation in the open ocean. *Deep-Sea Research, Part A: Oceanographic Research Papers*, *35*(4), 535–554. https://doi.org/10.1016/0198-0149(88)90130-6

Anderson, L. A. (1995). On the hydrogen and oxygen content of marine phytoplankton. *Deep Sea Research Part I: Oceanographic Research Papers*, *42*(9), 1675–1680. https://doi.org/10.1016/0967-0637(95)00072-E

Ascani, F., Richards, K. J., Firing, E., Grant, S., Johnson, K. S., Jia, Y., et al. (2013). Physical and biological controls of nitrate concentrations in the upper subtropical North Pacific Ocean. *Deep Sea Research Part II: Topical Studies in Oceanography*, *93*, 119–134. https://doi.org/10.1016/j.dsr2.2013.01.034

Barone, B., Church, M. J., Dugenne, M., Hawco, N. J., Jahn, O., White, A. E., et al. (2021). Biogeochemical observations in adjacent mesoscale eddies of opposite polarity (Version 1.0) [Dataset]. *Zenodo*. https://doi.org/10.5281/zenodo.5048504

Barone, B., Church, M. J., Dugenne, M., Hawco, N. J., Jahn, O., White, A. E., et al. (2022). Biogeochemical dynamics in adjacent mesoscale eddies of opposite polarity. *Global Biogeochemical Cycles*, *36*(2), e2021GB007115. https://doi.org/10.1029/2021GB007115

Barone, B., Coenen, A. R., Beckett, S. J., McGillicuddy, D. J., Weitz, J. S., & Karl, D. M. (2019). The ecological and biogeochemical state of the north pacific subtropical gyre is linked to sea surface height. *Journal of Marine Research*, *77*(2), 215–245. https://doi.org/10.1357/002224019828474241

Benitez-Nelson, C. R., Bidigare, R. R., Dickey, T. D., Landry, M. R., Leonard, C. L., Brown, S. L., et al. (2007). Mesoscale eddies drive increased silica export in the subtropical Pacific Ocean. *Science*, *316*(5827), 1017–1021. https://doi.org/10.1126/science.1136221

Bidigare, R. R., Benitez-Nelson, C., Leonard, C. L., Quay, P. D., Parsons, M. L., Foley, D. G., & Seki, M. P. (2003). Influence of a cyclonic eddy on microheterotroph biomass and carbon export in the lee of Hawaii. *Geophysical Research Letters*, *30*(6), 1318. https://doi.org/10.1029/2002GL016393

Böttjer, D., Dore, J. E., Karl, D. M., Letelier, R. M., Mahaffey, C., Wilson, S. T., et al. (2017). Temporal variability of nitrogen fixation and particulate nitrogen export at Station ALOHA. *Limnology & Oceanography*, *62*(1), 200–216. https://doi.org/10.1002/lno.10386

Boyd, P. W., Claustre, H., Levy, M., Siegel, D. A., & Weber, T. (2019). Multi-faceted particle pumps drive carbon sequestration in the ocean. *Nature*, *568*(7752), 327–335. https://doi.org/10.1038/s41586-019-1098-2

Briggs, N., Dall'Olmo, G., & Claustre, H. (2020). Major role of particle fragmentation in regulating biological sequestration of CO_2 by the oceans. *Science*, *367*(6479), 791–793. https://doi.org/10.1126/science.aay1790

Buesseler, K. O., Lamborg, C., Cai, P., Escoube, R., Johnson, R., Pike, S., et al. (2008). Particle fluxes associated with mesoscale eddies in the Sargasso Sea. *Deep-Sea Research Part II Topical Studies in Oceanography*, *55*(10–13), 1426–1444. https://doi.org/10.1016/j.dsr2.2008.02.007

Cao, H., Freilich, M., Song, X., Jing, Z., Fox-Kemper, B., Qiu, B., et al. (2024). Isopycnal submesoscale stirring crucially sustaining subsurface chlorophyll maximum in ocean cyclonic eddies. *Geophysical Research Letters*, *51*(4), e2023GL105793. https://doi.org/10.1029/2023GL105793

Carpenter, E. J., Harvey, H. R., Fry, B., & Capone, D. G. (1997). Biogeochemical tracers of the marine cyanobacterium Trichodesmium. *Deep Sea Research Part I: Oceanographic Research Papers*, *44*(1), 27–38. https://doi.org/10.1016/S0967-0637(96)00091-X

Carpenter, J. H. (1965). The accuracy of the winkler method for dissolved oxygen analysis. *Limnology & Oceanography*, *10*(1), 135–140. https://doi.org/10.4319/lo.1965.10.1.0135

Casciotti, K. L., Sigman, D. M., Hastings, M. G., Böhlke, J. K., & Hilkert, A. (2002). Measurement of the oxygen isotopic composition of nitrate in seawater and freshwater using the denitrifier method. *Analytical Chemistry*, *74*(19), 4905–4912. https://doi.org/10.1021/ac020113w

Casciotti, K. L., Trull, T. W., Glover, D. M., & Davies, D. (2008). Constraints on nitrogen cycling at the subtropical North Pacific Station ALOHA from isotopic measurements of nitrate and particulate nitrogen. *Deep-Sea Research Part II Topical Studies in Oceanography*, *55*(14–15), 1661–1672. https://doi.org/10.1016/j.dsr2.2008.04.017

Chelton, D. B., Schlax, M. G., & Samelson, R. M. (2011). Global observations of nonlinear mesoscale eddies. *Progress in Oceanography*, *91*(2), 167–216. https://doi.org/10.1016/j.pocean.2011.01.002

Church, M. J., Mahaffey, C., Letelier, R. M., Lukas, R., Zehr, J. P., & Karl, D. M. (2009). Physical forcing of nitrogen fixation and diazotroph community structure in the North Pacific subtropical gyre. *Global Biogeochemical Cycles*, *23*(2), GB2020. https://doi.org/10.1029/2008GB003418

Conway, T. M., Palter, J. B., & de Souza, G. F. (2018). Gulf Stream rings as a source of iron to the North Atlantic subtropical gyre. *Nature Geoscience*, *11*(8), 594–598. https://doi.org/10.1038/s41561-018-0162-0

Dabundo, R., Lehmann, M. F., Treibergs, L., Tobias, C. R., Altabet, M. A., Moisander, P. H., & Granger, J. (2014). The contamination of commercial 15N2 gas stocks with 15N–labeled nitrate and ammonium and consequences for nitrogen fixation measurements. *PLoS One*, *9*(10), e110335. https://doi.org/10.1371/journal.pone.0110335

Davis, C. S., & McGillicuddy, D. J. (2006). Transatlantic abundance of the N2-fixing colonial cyanobacterium Trichodesmium. *Science*, *312*(5779), 1517–1520. https://doi.org/10.1126/science.1123570

de Boyer Montégut, C., Madec, G., Fischer, A. S., Lazar, A., & Iudicone, D. (2004). Mixed layer depth over the global ocean: An examination of profile data and a profile-based climatology. *Journal of Geophysical Research*, *109*(C12), C12003. https://doi.org/10.1029/2004JC002378

Delwiche, C. C., Zinke, P. J., Johnson, C. M., & Virginia, R. A. (1979). Nitrogen isotope distribution as a presumptive indicator of nitrogen fixation. *Botanical Gazette*, *140*, S65–S69. https://doi.org/10.1086/337037

DeVries, T., Primeau, F., & Deutsch, C. (2012). The sequestration efficiency of the biological pump. *Geophysical Research Letters*, *39*(13), L13601. https://doi.org/10.1029/2012GL051963

DeVries, T., & Weber, T. (2017). The export and fate of organic matter in the ocean: New constraints from combining satellite and oceanographic tracer observations. *Global Biogeochemical Cycles*, *31*(3), 535–555. https://doi.org/10.1002/2016GB005551

Dong, C., McWilliams, J. C., Liu, Y., & Chen, D. (2014). Global heat and salt transports by eddy movement. *Nature Communications*, *5*, 1–6. https://doi.org/10.1038/ncomms4294

Dore, J. E., Brum, J. R., Tupas, L. M., & Karl, D. M. (2002). Seasonal and interannual variability in sources of nitrogen supporting export in the oligotrophic subtropical North Pacific Ocean. *Limnology & Oceanography*, *47*(6), 1595–1607. https://doi.org/10.4319/lo.2002.47.6.1595

Dore, J. E., Houlihan, T., Hebel, D. V., Tien, G., Tupas, L., & Karl, D. M. (1996). Freezing as a method of sample preservation for the analysis of dissolved inorganic nutrients in seawater. *Marine Chemistry*, *53*(3–4), 173–185. https://doi.org/10.1016/0304-4203(96)00004-7

Dore, J. E., Letelier, R. M., Church, M. J., Lukas, R., & Karl, D. M. (2008). Summer phytoplankton blooms in the oligotrophic North Pacific Subtropical Gyre: Historical perspective and recent observations. *Progress in Oceanography*, *76*(1), 2–38. https://doi.org/10.1016/j.pocean.2007.10.002

D'Ovidio, F., De Monte, S., Penna, A. D., Cotté, C., & Guinet, C. (2013). Ecological implications of eddy retention in the open ocean: A Lagrangian approach. *Journal of Physics A: Mathematical and Theoretical*, *46*(25), 1–22. https://doi.org/10.1088/1751-8113/46/25/254023

Dugenne, M., Gradoville, M. R., Church, M. J., Wilson, S. T., Sheyn, U., Harke, M. J., et al. (2023). Nitrogen fixation in mesoscale eddies of the North Pacific subtropical gyre: Patterns and mechanisms. *Global Biogeochemical Cycles*, *37*(4), e2022GB007386. https://doi.org/10.1029/2022GB007386

Early, J. J., Samelson, R. M., & Chelton, D. B. (2011). The evolution and propagation of quasigeostrophic ocean eddies. *Journal of Physical Oceanography*, *41*(8), 1535–1555. https://doi.org/10.1175/2011JPO4601.1

Emerson, S., & Hayward, T. L. (1995). Chemical tracers of biological processes in shallow waters of North Pacific: Preformed nitrate distributions (pp. 499–513).

Falkowski, P. G., Ziemann, D., Kolber, Z., & Bienfangt, P. K. (1991). 352055a0. *Role of Eddy Pumping in Enhancing Primary Production in the Ocean*, *352*(July), 55–58. https://doi.org/10.1038/352055a0

Fawcett, S. E., Johnson, K. S., Riser, S. C., Oostende, N. V., & Sigman, D. M. (2018). Low-nutrient organic matter in the Sargasso Sea thermocline: A hypothesis for its role, identity, and carbon cycle implications. *Marine Chemistry*, *207*(April), 108–123. https://doi.org/10.1016/j.marchem.2018.10.008

Fawcett, S. E., Lomas, M. W., Casey, J. R., Ward, B. B., & Sigman, D. M. (2011). Assimilation of upwelled nitrate by small eukaryotes in the Sargasso Sea. *Nature Geoscience*, *4*(10), 717–722. https://doi.org/10.1038/ngeo1265

Fawcett, S. E., Ward, B. B., Lomas, M. W., & Sigman, D. M. (2015). Vertical decoupling of nitrate assimilation and nitrification in the Sargasso Sea. *Deep-Sea Research Part I Oceanographic Research Papers*, *103*, 64–72. https://doi.org/10.1016/j.dsr.2015.05.004

Flierl, G. R. (1981). Particle motions in large-amplitude wave fields. *Geophysical & Astrophysical Fluid Dynamics*, *18*(1–2), 39–74. https://doi.org/10.1080/03091928108208773

Fong, A. A., Karl, D. M., Lukas, R., Letelier, R. M., Zehr, J. P., & Church, M. J. (2008). Nitrogen fixation in an anticyclonic eddy in the oligotrophic North Pac. *ISME Journal*, *2*(6), 663–676. https://doi.org/10.1038/ismej.2008.22

Foreman, R. K., Segura-Noguera, M., & Karl, D. M. (2016). Validation of Ti(III) as a reducing agent in the chemiluminescent determination of nitrate and nitrite in seawater. *Marine Chemistry*, *186*, 83–89. https://doi.org/10.1016/j.marchem.2016.08.003

Freilich, M. A., & Mahadevan, A. (2019). Decomposition of vertical velocity for nutrient transport in the upper ocean. *Journal of Physical Oceanography*, *49*(6), 1561–1575. https://doi.org/10.1175/JPO-D-19-0002.1

Gaube, P., Chelton, D. B., Strutton, P. G., & Behrenfeld, M. J. (2013). Satellite observations of chlorophyll, phytoplankton biomass, and Ekman pumping in nonlinear mesoscale eddies. *Journal of Geophysical Research: Oceans*, *118*(12), 6349–6370. https://doi.org/10.1002/2013JC009027

Gaube, P., McGillicuddy, D. J., Chelton, D. B., Behrenfeld, M. J., & Strutton, P. G. (2014). Regional variations in the influence of mesoscale eddies on near-surface chlorophyll. *Journal of Geophysical Research: Oceans*, *119*(12), 8195–8220. https://doi.org/10.1002/2014JC010111

Granger, J., Sigman, D. M., Rohde, M. M., Maldonado, M. T., & Tortell, P. D. (2010). N and O isotope effects during nitrate assimilation by unicellular prokaryotic and eukaryotic plankton cultures. *Geochimica et Cosmochimica Acta*, *74*(3), 1030–1040. https://doi.org/10.1016/j.gca.2009.10.044

Guidi, L., Calil, P. H. R., Duhamel, S., Björkman, K. M., Doney, S. C., Jackson, G. A., et al. (2012). Does eddy-eddy interaction control surface phytoplankton distribution and carbon export in the North Pacific Subtropical Gyre? *Journal of Geophysical Research*, *117*(G2), G02024. https://doi.org/10.1029/2012JG001984

Guo, M., Xing, X., Xiu, P., Dall'Olmo, G., Chen, W., & Chai, F. (2024). Efficient biological carbon export to the mesopelagic ocean induced by submesoscale fronts. *Nature Communications*, *15*(1), 580. https://doi.org/10.1038/s41467-024-44846-7

Gupta, M., Williams, R. G., Lauderdale, J. M., Jahn, O., Hill, C., Dutkiewicz, S., & Follows, M. J. (2022). A nutrient relay sustains subtropical ocean productivity. *Proceedings of the National Academy of Sciences of the United States of America*, *119*(41). https://doi.org/10.1073/pnas.2206504119

Hannides, C. C. S., Popp, B. N., Choy, C. A., & Drazen, J. C. (2013). Midwater zooplankton and suspended particle dynamics in the North Pacific Subtropical Gyre: A stable isotope perspective. *Limnology & Oceanography*, *58*(6), 1931–1946. https://doi.org/10.4319/lo.2013.58.6.1931

Hawco, N. J., Barone, B., Church, M. J., Babcock-Adams, L., Repeta, D. J., Wear, E. K., et al. (2021). Iron depletion in the deep chlorophyll maximum: Mesoscale eddies as natural iron fertilization experiments. *Global Biogeochemical Cycles*, *35*(12), e2021GB007112. https://doi.org/10.1029/2021GB007112

Hoering, T. C., & Ford, H. T. (1960). The isotope effect in the fixation of nitrogen by Azotobacter. *Journal of the American Chemical Society*, *82*(2), 376–378. https://doi.org/10.1021/ja01487a031

HOT-DOGS. (2024). The Hawaii ocean time-series data organization & graphical system [Dataset]. *HOT-DOGS*. Retrieved from https://hahana.soest.hawaii.edu/hot/hot-dogs/interface.html

Johnson, K. S., Riser, S. C., & Karl, D. M. (2010). Nitrate supply from deep to near-surface waters of the North Pacific subtropical gyre. *Nature*, *465*(7301), 1062–1065. https://doi.org/10.1038/nature09170

Karl, D., Letelier, R., Tupas, L., Dore, J., Christian, J., & Hebel, D. (1997). The role of nitrogen fixation in biogeochemical cycling in the subtropical North Pacific Ocean. *Nature*, *388*(6642), 533–538. https://doi.org/10.1038/41474

Karl, D. M. (1999). A sea of change: Biogeochemical variability in the North Pacific Subtropical Gyre. *Ecosystems*, *2*(3), 181–214. https://doi.org/10.1007/s100219900068

Karl, D. M., & Church, M. J. (2017). Ecosystem structure and dynamics in the North Pacific subtropical gyre: New views of an old ocean. *Ecosystems*, *20*(3), 433–457. https://doi.org/10.1007/s10021-017-0117-0

Karl, D. M., Church, M. J., Dore, J. E., Letelier, R. M., & Mahaffey, C. (2012). Predictable and efficient carbon sequestration in the North Pacific Ocean supported by symbiotic nitrogen fixation. *Proceedings of the National Academy of Sciences*, *109*(6), 1842–1849. https://doi.org/10.1073/pnas.1120312109

Karl, D. M., & Lukas, R. (1996). The Hawaii ocean time-series (HOT) program: Background, rationale and field implementation. *Deep Sea Research Part II: Topical Studies in Oceanography*, *43*(2–3), 129–156. https://doi.org/10.1016/0967-0645(96)00005-7

Knapp, A. N., Casciotti, K. L., Berelson, W. M., Prokopenko, M. G., & Capone, D. G. (2016). Low rates of nitrogen fixation in eastern tropical South Pacific surface waters. *Proceedings of the National Academy of Sciences*, *113*(16), 4398–4403. https://doi.org/10.1073/pnas.1515641113

Knapp, A. N., DiFiore, P. J., Deutsch, C., Sigman, D. M., & Lipschultz, F. (2008). Nitrate isotopic composition between Bermuda and Puerto Rico: Implications for N_2 fixation in the Atlantic Ocean. *Global Biogeochemical Cycles*, *22*(3), GB3014. https://doi.org/10.1029/2007GB003107

Knapp, A. N., McCabe, K. M., Grosso, O., Leblond, N., Moutin, T., & Bonnet, S. (2018). Distribution and rates of nitrogen fixation in the western tropical South Pacific Ocean constrained by nitrogen isotope budgets. *Biogeosciences*, *15*(9), 2619–2628. https://doi.org/10.5194/bg-15-2619-2018

Knapp, A. N., Sigman, D. M., & Lipschultz, F. (2005). N isotopic composition of dissolved organic nitrogen and nitrate at the Bermuda Atlantic Time-series study site. *Global Biogeochemical Cycles*, *19*(1), 1–15. https://doi.org/10.1029/2004GB002320

Knapp, A. N., Sigman, D. M., Lipschultz, F., Kustka, A. B., & Capone, D. G. (2011). Interbasin isotopic correspondence between upper-ocean bulk DON and subsurface nitrate and its implications for marine nitrogen cycling. *Global Biogeochemical Cycles*, *25*(4), GB4004. https://doi.org/10.1029/2010GB003878

Knauer, G. A., Martin, J. H., & Bruland, K. W. (1979). Fluxes of particulate carbon, nitrogen, and phosphorus in the upper water column of the northeast Pacific. *Deep-Sea Research, Part A: Oceanographic Research Papers*, *26*(1), 97–108. https://doi.org/10.1016/0198-0149(79)90089-X

Lampitt, R. S., Noji, T., & von Bodungen, B. (1990). What happens to zooplankton faecal pellets? Implications for material flux. *Marine Biology*, *104*(1), 15–23. https://doi.org/10.1007/BF01313152

Lehmann, M. F., Bernasconi, S. M., Barbieri, A., & McKenzie, J. A. (2002). Preservation of organic matter and alteration of its carbon and nitrogen isotope composition during simulated and in situ early sedimentary diagenesis. *Geochimica et Cosmochimica Acta*, *66*(20), 3573–3584. https://doi.org/10.1016/S0016-7037(02)00968-7

Lehmann, N., Granger, J., Kienast, M., Brown, K. S., Rafter, P. A., Martínez-Méndez, G., & Mohtadi, M. (2018). Isotopic evidence for the evolution of subsurface nitrate in the western equatorial Pacific. *Journal of Geophysical Research: Oceans*, *123*(3), 1684–1707. https://doi.org/10.1002/2017JC013527

Letelier, R. M., Karl, D. M., Abbott, M. R., & Bidigare, R. R. (2004). Light driven seasonal patterns of chlorophyll and nitrate in the lower euphotic zone of the North Pacific Subtropical Gyre. *Limnology & Oceanography*, *49*(2), 508–519. https://doi.org/10.4319/lo.2004.49.2.0508

Letelier, R. M., Karl, D. M., Abbott, M. R., Flament, P., Freilich, M., Lukas, R., & Strub, T. (2000). Role of late winter mesoscale events in the biogeochemical variability of the upper water column of the North Pacific Subtropical Gyre. *Journal of Geophysical Research*, *105*(C12), 28723–28739. https://doi.org/10.1029/1999JC000306

Letscher, R. T., Knapp, A. N., James, A. K., Carlson, C. A., Santoro, A. E., & Hansell, D. A. (2015). Microbial community composition and nitrogen availability influence DOC remineralization in the South Pacific Gyre. *Marine Chemistry*, *177*, 325–334. https://doi.org/10.1016/j.marchem.2015.06.024

Letscher, R. T., & Villareal, T. A. (2018). Evaluation of the seasonal formation of subsurface negative preformed nitrate anomalies in the subtropical North Pacific and North Atlantic. *Biogeosciences*, *3*, 6461–6480.

Lévy, M., Ferrari, R., Franks, P. J. S., Martin, A. P., & Rivière, P. (2012). Bringing physics to life at the submesoscale. *Geophysical Research Letters*, *39*(14), L14602. https://doi.org/10.1029/2012GL052756

Li, G., Cheng, L., Zhu, J., Trenberth, K. E., Mann, M. E., & Abraham, J. P. (2020). Increasing ocean stratification over the past half-century. *Nature Climate Change*, *10*(12), 1116–1123. https://doi.org/10.1038/s41558-020-00918-2

Liu, J., Zhou, L., Li, J., Lin, Y., Ke, Z., Zhao, C., et al. (2020). Effect of mesoscale eddies on diazotroph community structure and nitrogen fixation rates in the South China Sea. *Regional Studies in Marine Science*, *35*, 101106. https://doi.org/10.1016/j.rsma.2020.101106

Liu, K.-K., Su, M.-J., Hsueh, C.-R., & Gong, G.-C. (1996). The nitrogen isotopic composition of nitrate in the Kuroshio Water northeast of Taiwan: Evidence for nitrogen fixation as a source of isotopically light nitrate. *Marine Chemistry*, *54*(3–4), 273–292. https://doi.org/10.1016/0304-4203(96)00034-5

Löscher, C. R., Bourbonnais, A., Dekaezemacker, J., Charoenpong, C. N., Altabet, M. A., Bange, H. W., et al. (2016). N2 fixation in eddies of the eastern tropical South Pacific Ocean. *Biogeosciences*, *13*(10), 2889–2899. https://doi.org/10.5194/bg-13-2889-2016

Lovecchio, E., Gruber, N., Münnich, M., & Frenger, I. (2022). On the processes sustaining biological production in the offshore propagating eddies of the Northern Canary upwelling system. *Journal of Geophysical Research: Oceans*, *127*(2), e2021JC017691. https://doi.org/10.1029/2021JC017691

Mahaffey, C., Benitez-Nelson, C. R., Bidigare, R. R., Rii, Y., & Karl, D. M. (2008). Nitrogen dynamics within a wind-driven eddy. *Deep-Sea Research Part II Topical Studies in Oceanography*, *55*(10–13), 1398–1411. https://doi.org/10.1016/j.dsr2.2008.02.004

Maiti, K., Benitez-Nelson, C. R., Rii, Y., & Bidigare, R. (2008). The influence of a mature cyclonic eddy on particle export in the lee of Hawaii. *Deep-Sea Research Part II Topical Studies in Oceanography*, *55*(10–13), 1445–1460. https://doi.org/10.1016/j.dsr2.2008.02.008

Marconi, D., Sigman, D. M., Casciotti, K. L., Campbell, E. C., Alexandra Weigand, M., Fawcett, S. E., et al. (2017). Tropical dominance of N_2 fixation in the North Atlantic Ocean. *Global Biogeochemical Cycles*, *31*(10), 1608–1623. https://doi.org/10.1002/2016GB005613

Marsay, C. M., Sanders, R. J., Henson, S. A., Pabortsava, K., Achterberg, E. P., & Lampitt, R. S. (2015). Attenuation of sinking particulate organic carbon flux through the mesopelagic ocean. *Proceedings of the National Academy of Sciences*, *112*(4), 1089–1094. https://doi.org/10.1073/pnas.1415311112

Marshall, T., Granger, J., Casciotti, K. L., Dähnke, K., Emeis, K.-C., Marconi, D., et al. (2022). The Angola Gyre is a hotspot of dinitrogen fixation in the South Atlantic Ocean. *Communications Earth & Environment*, *3*(1), 151. https://doi.org/10.1038/s43247-022-00474-x

Marshall, T. A., Sigman, D. M., Beal, L. M., Foreman, A., Martínez-García, A., Blain, S., et al. (2023). The Agulhas current transports signals of local and remote Indian Ocean nitrogen cycling. *Journal of Geophysical Research: Oceans*, *128*(3), e2022JC019413. https://doi.org/10.1029/2022JC019413

McCave, I. N. (1975). Vertical flux of particles in the ocean. *Deep-Sea Research and Oceanographic Abstracts*, *22*(7), 491–502. https://doi.org/10.1016/0011-7471(75)90022-4

McGillicuddy, D. J. (2016). Mechanisms of physical-biological-biogeochemical interaction at the oceanic mesoscale. *Annual Review of Marine Science*, *8*(1), 125–159. https://doi.org/10.1146/annurev-marine-010814-015606

McGillicuddy, D. J., & Robinson, A. R. (1997). Eddy-induced nutrient supply and new production in the Sargasso Sea. *Deep Sea Research Part I: Oceanographic Research Papers*, *44*(8), 1427–1450. https://doi.org/10.1016/S0967-0637(97)00024-1

McGillicuddy, D. J., Robinson, A. R., Siegel, D. A., Jannasch, H. W., Johnson, R., Dickey, T. D., et al. (1998). Influence of mesoscale eddies on new production in the Sargasso Sea. *Nature*, *394*(6690), 263–266. https://doi.org/10.1038/28367

McIlvin, M. R., & Casciotti, K. L. (2011). Technical updates to the bacterial method for nitrate isotopic analyses. *Analytical Chemistry*, *83*(5), 1850–1856. https://doi.org/10.1021/ac1028984

Minagawa, M., & Wada, E. (1986). Nitrogen isotope ratios of red tide organisms in the East China Sea: A characterization of biological nitrogen fixation. *Marine Chemistry*, *19*(3), 245–259. https://doi.org/10.1016/0304-4203(86)90026-5

Mohr, W., Großkopf, T., Wallace, D. W. R., & LaRoche, J. (2010). Methodological underestimation of oceanic nitrogen fixation rates. *PLoS One*, *5*(9), 1–7. https://doi.org/10.1371/journal.pone.0012583

Nicholson, D., Emerson, S., & Eriksen, C. C. (2008). Net community production in the deep euphotic zone of the subtropical North Pacific gyre from glider surveys. *Limnology & Oceanography*, *53*(5 PART 2), 2226–2236. https://doi.org/10.4319/lo.2008.53.5_part_2.2226

Okubo, A. (1971). Oceanic diffusion diagrams. *Deep-Sea Research and Oceanographic Abstracts*, *18*(8), 789–802. https://doi.org/10.1016/0011-7471(71)90046-5

Omand, M. M., D'Asaro, E. A., Lee, C. M., Perry, M. J., Briggs, N., Cetinić, I., & Mahadevan, A. (2015). Eddy-driven subduction exports particulate organic carbon from the spring bloom. *Science*, *348*(6231), 222–225. https://doi.org/10.1126/science.1260062

Omand, M. M., Govindarajan, R., He, J., & Mahadevan, A. (2020). Sinking flux of particulate organic matter in the oceans: Sensitivity to particle characteristics. *Scientific Reports*, *10*(1), 5582. https://doi.org/10.1038/s41598-020-60424-5

Pegliasco, C., Busché, C., & Faugère, Y. (2022). Mesoscale eddy trajectory atlas META3.2 delayed-time all satellites: Version META3.2 DT allsat [Dataset]. *HOT-DOGS*. https://doi.org/10.24400/527896/A01-2022.005.220209

Polovina, J. J., Howell, E. A., & Abecassis, M. (2008). Ocean's least productive waters are expanding. *Geophysical Research Letters*, *35*(3), L03618. https://doi.org/10.1029/2007GL031745

Resplandy, L., Lévy, M., & McGillicuddy, D. J. (2019). Effects of eddy-driven subduction on ocean biological carbon pump. *Global Biogeochemical Cycles*, *33*(8), 1071–1084. https://doi.org/10.1029/2018GB006125

Rii, Y. M., Brown, S. L., Nencioli, F., Kuwahara, V., Dickey, T., Karl, D. M., & Bidigare, R. R. (2008). The transient oasis: Nutrient-phytoplankton dynamics and particle export in Hawaiian lee cyclones. *Deep-Sea Research Part II Topical Studies in Oceanography*, *55*(10–13), 1275–1290. https://doi.org/10.1016/j.dsr2.2008.01.013

Sabine, C. L., Mackenzie, F. T., Winn, C., & Karl, D. M. (1995). Geochemistry of carbon dioxide in seawater at the Hawaii Ocean Time Series Station, ALOHA. *Global Biogeochemical Cycles*, *9*(4), 637–651. https://doi.org/10.1029/95GB02382

Sallée, J.-B., Pellichero, V., Akhoudas, C., Pauthenet, E., Vignes, L., Schmidtko, S., et al. (2021). Summertime increases in upper-ocean stratification and mixed-layer depth. *Nature*, *591*(7851), 592–598. https://doi.org/10.1038/s41586-021-03303-x

Seki, M. P., Polovina, J. J., Brainard, R. E., Bidigare, R. R., Leonard, C. L., & Foley, D. G. (2001). Biological enhancement at cyclonic eddies tracked with GOES thermal imagery in Hawaiian waters. *Geophysical Research Letters*, *28*(8), 1583–1586. https://doi.org/10.1029/2000GL012439

Shcherbina, A. Y., Sundermeyer, M. A., Kunze, E., D'Asaro, E., Badin, G., Birch, D., et al. (2015). The LatMix summer campaign: Submesoscale stirring in the upper ocean. *Bulletin of the American Meteorological Society*, *96*(8), 1257–1279. https://doi.org/10.1175/BAMS-D-14-00015.1

Siegel, D. A., McGillicuddy, D. J., & Fields, E. A. (1999). Mesoscale eddies, satellite altimetry, and new production in the Sargasso Sea. *Journal of Geophysical Research*, *104*(C6), 13359–13379. https://doi.org/10.1029/1999jc900051

Sigman, D. M., Casciotti, K. L., Andreani, M., Barford, C., Galanter, M., & Böhlke, J. K. (2001). A bacterial method for the nitrogen isotopic analysis of nitrate in seawater and freshwater. *Analytical Chemistry*, *73*(17), 4145–4153. https://doi.org/10.1021/ac010088e

Sigman, D. M., DiFiore, P. J., Hain, M. P., Deutsch, C., & Karl, D. M. (2009). Sinking organic matter spreads the nitrogen isotope signal of pelagic denitrification in the North Pacific. *Geophysical Research Letters*, *36*(8), L08605. https://doi.org/10.1029/2008GL035784

Smyth, A. J., & Letscher, R. T. (2023). Spatial and temporal occurrence of preformed nitrate anomalies in the subtropical North Pacific and North Atlantic oceans. *Marine Chemistry*, *252*, 104248. https://doi.org/10.1016/j.marchem.2023.104248

Spingys, C. P., Williams, R. G., Tuerena, R. E., Naveira Garabato, A., Vic, C., Forryan, A., & Sharples, J. (2021). Observations of nutrient supply by mesoscale eddy stirring and small-scale turbulence in the oligotrophic North Atlantic. *Global Biogeochemical Cycles*, *35*(12), 1–20. https://doi.org/10.1029/2021GB007200

Stukel, M. R., Aluwihare, L. I., Barbeau, K. A., Chekalyuk, A. M., Goericke, R., Miller, A. J., et al. (2017). Mesoscale ocean fronts enhance carbon export due to gravitational sinking and subduction. *Proceedings of the National Academy of Sciences*, *114*(6), 1252–1257. https://doi.org/10.1073/pnas.1609435114

Talley, L. D. (1985). Ventilation of the subtropical North Pacific: The shallow salinity minimum. *Journal of Physical Oceanography*, *15*(6), 633–649. https://doi.org/10.1175/1520-0485(1985)015<0633:VOTSNP>2.0.CO;2

Talley, L. D. (1993). Distribution and formation of north pacific intermediate water. *Journal of Physical Oceanography*, *23*(3), 517–537. https://doi.org/10.1175/1520-0485(1993)023<0517:DAFONP>2.0.CO;2

Tsuchiya, M. (1968). Upper waters of the intertropical Pacific Ocean. *Johns Hopkins Oceanographic Studies*, *4*, 50.

Tupas, L., Santiago-Mandujano, F., & Lukas, R. (1997). *Hawaii ocean time-series data report 8: 1996*. University of Hawaii School of Ocean and Earth Science and Technology.

Villareal, T. A., Pilskaln, C., Brzezinski, M., Lipschultz, F., Dennett, M., & Gardner, G. B. (1999). Upward transport of oceanic nitrate by migrating diatom mats. *Nature*, *397*(6718), 423–425. https://doi.org/10.1038/17103

Washburn, L., Siegel, D. A., Dickey, T. D., & Hamilton, M. K. (1989). Isopycnal mixing and the distribution of particles across the North Pacific Subtropical Front. *Deep-Sea Research, Part A: Oceanographic Research Papers*, *36*(11), 1607–1620. https://doi.org/10.1016/0198-0149(89)90062-9

Weber, T., Cram, J. A., Leung, S. W., DeVries, T., & Deutsch, C. (2016). Deep ocean nutrients imply large latitudinal variation in particle transfer efficiency. *Proceedings of the National Academy of Sciences*, *113*(31), 8606–8611. https://doi.org/10.1073/pnas.1604414113

Weigand, M. A., Foriel, J., Barnett, B., Oleynik, S., & Sigman, D. M. (2016). Updates to instrumentation and protocols for isotopic analysis of nitrate by the denitrifier method. *Rapid Communications in Mass Spectrometry*, *30*(12), 1365–1383. https://doi.org/10.1002/rcm.7570

White, A. E., Granger, J., Selden, C., Gradoville, M. R., Potts, L., Bourbonnais, A., et al. (2020). A critical review of the $15N_2$ tracer method to measure diazotrophic production in pelagic ecosystems. *Limnology and Oceanography: Methods*, *18*(4), 129–147. https://doi.org/10.1002/lom3.10353

Wilson, S. E., Steinberg, D. K., & Buesseler, K. O. (2008). Changes in fecal pellet characteristics with depth as indicators of zooplankton repackaging of particles in the mesopelagic zone of the subtropical and subarctic North Pacific Ocean. *Deep Sea Research Part II: Topical Studies in Oceanography*, *55*(14–15), 1636–1647. https://doi.org/10.1016/j.dsr2.2008.04.019

Xiu, P., & Chai, F. (2020). Eddies affect subsurface phytoplankton and oxygen distributions in the North Pacific subtropical gyre. *Geophysical Research Letters*, *47*(15), e2020GL087037. https://doi.org/10.1029/2020GL087037

Yuan, Z., Browning, T. J., Du, C., Shen, H., Wang, L., Ma, Y., et al. (2023). Enhanced phosphate consumption stimulated by nitrogen fixation within a cyclonic eddy in the northwest Pacific. *Journal of Geophysical Research: Oceans*, *128*(11), e2023JC019947. https://doi.org/10.1029/2023JC019947

Zhang, Z., Wang, W., & Qiu, B. (2014). Oceanic mass transport by mesoscale eddies. *Science*, *345*(6194), 322–324. https://doi.org/10.1126/science.1252418

Zhou, K., Benitez-Nelson, C. R., Huang, J., Xiu, P., Sun, Z., & Dai, M. (2021). Cyclonic eddies modulate temporal and spatial decoupling of particulate carbon, nitrogen, and biogenic silica export in the North Pacific Subtropical Gyre. *Limnology & Oceanography*, *66*(9), 3508–3522. https://doi.org/10.1002/lno.11895

Zhou, K., Dai, M., Xiu, P., Wang, L., Hu, J., & Benitez-Nelson, C. R. (2020). Transient enhancement and decoupling of carbon and opal export in cyclonic eddies. *Journal of Geophysical Research: Oceans*, *125*(9), e2020JC016372. https://doi.org/10.1029/2020JC016372

Zhou, M., Granger, J., & Chang, B. X. (2022). Influence of sample volume on nitrate N and O isotope ratio analyses with the denitrifier method. *Rapid Communications in Mass Spectrometry*, *36*(4). https://doi.org/10.1002/rcm.9224

Zhou, M., Granger, J., Barone, B., & White, A. E. (2025). Nitrate 15N/14N measurements in two adjacent mesoscale eddies in the North Pacific Subtropical Gyre from water samples collected on R/V Kilo Moana cruise KM1709 in June-July 2017 (Version 1) [Dataset]. *Biological and Chemical Oceanography Data Management Office (BCO-DMO)*. https://doi.org/10.26008/1912/BCO-DMO.948358.1

Zhu, X.-Y., Yang, Z., Xie, Y., Zhou, K., & Wang, W.-L. (2023). Strong particle dynamics counteract the nutrient-pumping effect leading to weak carbon flux in a cyclonic eddy. *Marine Chemistry*, *255*, 104279. https://doi.org/10.1016/j.marchem.2023.104279

References From the Supporting Information

Chaigneau, A., Le Texier, M., Eldin, G., Grados, C., & Pizarro, O. (2011). Vertical structure of mesoscale eddies in the eastern South Pacific Ocean: A composite analysis from altimetry and Argo profiling floats. *Journal of Geophysical Research*, *116*(C11), C11025. https://doi.org/10.1029/2011JC007134

Chelton, D. B., Schlax, M. G., Samelson, R. M., & de Szoeke, R. A. (2007). Global observations of large oceanic eddies. *Geophysical Research Letters*, *34*(15), L15606. https://doi.org/10.1029/2007GL030812

Eppley, R. W., & Peterson, B. J. (1979). Particulate organic matter flux and planktonic new production in the deep ocean. *Nature*, *282*(5740), 677–680. https://doi.org/10.1038/282677a0